Journal of Nonlinear Science (2024) 34:86
https://doi.org/10.1007/s00332-024-10064-0

Journal of Nonlinear Science

# Axisymmetric Flows with Swirl for Euler and Navier–Stokes Equations

**Theodoros Katsaounis[1,2] · Ioanna Mousikou[3] · Athanasios E. Tzavaras[3]**

Received: 11 November 2023 / Accepted: 26 June 2024 / Published online: 15 July 2024


## Abstract

We consider the incompressible axisymmetric Navier–Stokes equations with swirl as an idealized model for tornado-like flows. Assuming an infinite vortex line which interacts with a boundary surface resembles the tornado core, we look for stationary self-similar solutions of the axisymmetric Euler and axisymmetric Navier–Stokes equations. We are particularly interested in the connection of the two problems in the zero-viscosity limit. First, we construct a class of explicit stationary self-similar solutions for the axisymmetric Euler equations. Second, we consider the possibility of discontinuous solutions and prove that there do not exist self-similar stationary Euler solutions with slip discontinuity. This nonexistence result is extended to a class of flows where there is mass input or mass loss through the vortex core. Third, we consider solutions of the Euler equations as zero-viscosity limits of solutions to Navier–Stokes. Using techniques from the theory of Riemann problems for conservation laws, we prove that, under certain assumptions, stationary self-similar solutions of the axisymmetric Navier–Stokes equations converge to stationary self-similar solutions of the axisymmetric Euler equations as $\nu \to 0$. This allows to characterize the type of Euler solutions that arise via viscosity limits.

Communicated by Jean-Luc Thiffeault.

✉ Athanasios E. Tzavaras
athanasios.tzavaras@kaust.edu.sa

Theodoros Katsaounis
thodoros.katsaounis@uoc.gr

Ioanna Mousikou
ioanna.mousikou@kaust.edu.sa

[1] Department of Mathematics and Applied Mathematics, University of Crete, 70013 Heraklion, Crete, Greece

[2] Institute of Applied and Computational Mathematics, FORTH, Heraklion, Greece

[3] Computer, Electrical, Mathematical Sciences and Engineering Division, King Abdullah University of Science and Technology (KAUST), Thuwal, Saudi Arabia

**Keywords** Tornadoes · Axisymmetric flows with swirl · Incompressible Navier-Stokes · Interaction of vortex with boundary · Self-similar flows · Stationary solutions of Euler arising via viscosity

**Mathematics Subject Classification** 76B47 · 76D10 · 76D17 · 35C06 · 35Q30

## Contents



## 1 Introduction

Tornadoes are among the most extreme and destructive weather phenomena, and due to the numerous casualties and substantial damage in property, their modelling has attracted considerable interest. At the core of mathematical models for the description of tornadoes is the concept of swirling flows. Assuming the tornado structure does not change significantly in time and that a vortex line resembles the tornado core, Morton (1966), a common model for tornado-like flows is the stationary incompressible axisymmetric Navier–Stokes equations. Namely, the following system in cylindrical coordinates is considered

$$u\frac{\partial u}{\partial r}+w\frac{\partial u}{\partial z}-\frac{v^2}{r}=\nu\Big[\frac{1}{r}\frac{\partial}{\partial r}\Big(r\frac{\partial u}{\partial r}\Big)+\frac{\partial^2 u}{\partial z^2}-\frac{u}{r^2}\Big]-\frac{\partial p}{\partial r}, \tag{1.1a}$$

$$u\frac{\partial v}{\partial r}+w\frac{\partial v}{\partial z}+\frac{uv}{r}=\nu\Big[\frac{1}{r}\frac{\partial}{\partial r}\Big(r\frac{\partial v}{\partial r}\Big)+\frac{\partial^2 v}{\partial z^2}-\frac{v}{r^2}\Big], \tag{1.1b}$$

$$u\frac{\partial w}{\partial r}+w\frac{\partial w}{\partial z}=\nu\Big[\frac{1}{r}\frac{\partial}{\partial r}\Big(r\frac{\partial w}{\partial r}\Big)+\frac{\partial^2 w}{\partial z^2}\Big]-\frac{\partial p}{\partial z}, \tag{1.1c}$$

$$\frac{1}{r}\frac{\partial}{\partial r}(ru)+\frac{\partial w}{\partial z}=0, \tag{1.1d}$$

where $\vec{u}=(u,v,w):\mathbb{R}^3\times\mathbb{R}_+\to\mathbb{R}^3$ is the velocity, $p:\mathbb{R}^3\times\mathbb{R}_+\to\mathbb{R}$ is the pressure, and $\nu\geq 0$ is the coefficient of kinematic viscosity. Modelling tornadoes necessitates the consideration of certain additional factors, like rotation induced from the cloud and buoyancy effects. The reader is referred to "' B" for a quick presentation of models and references. Nevertheless, system (1.1) is considered as the base model for describing their core structure, Rotunno (2013).

Long (1958, 1961) introduced a self-similar ansatz and reduced the stationary axisymmetric Navier–Stokes equations to a system of ordinary differential equations focusing on the boundary layer description. Independently, Goldshtik (1960) examined the existence of self-similar solutions as the Reynolds number varies; he concluded his system is not solvable for all Reynolds numbers and characterized this loss of existence as a 'paradox'. Few years later, Serrin (1972) presented another self-similar ansatz and showed that only three types of solution can be associated with the interaction of an infinite vortex line with a boundary plane: the flow can be either ascending, or descending, or a combination of these two profiles, i.e. downwards near the vortex line and inwards near the r-axis. The latter is usually referred as a double-celled vortex, and Serrin (1972) presented extensive comparisons of such solutions to tornadoes.

Many authors subsequently studied the system (1.1) on occasion considering more general families of self-similar solutions, for example (Fernandez-Feria et al. 1995; Bělík et al. 2014; Goldshtik and Shtern 1990), or more general geometries including for example conical flows, Goldshtik and Shtern (1990), Goldshtik (1990), Sozou (1992), Sozou et al. (1994), Fernandez-Feria and Arrese (2000), Shtern (2012).

This work has two objectives: First, to consider the full system (1.1) and provide a complete study of the stationary self-similar solutions of axisymmetric Navier–Stokes and of axisymmetric Euler equations. Second, to compare those equations and study the emergence of Euler solutions from the Navier–Stokes solutions as the viscosity $\nu$ goes to zero. One novel feature for the Euler equations is the consideration of solutions with a slip discontinuity in the velocities. Regarding the Navier–Stokes equations, we obtain an alternative derivation of the equations studied by Serrin (1972) and study the emergence of stationary self-similar solutions of the Euler equations as zero-viscosity limits from corresponding solutions of the Navier–Stokes equations. The goal is to check whether the two-celled solutions identified in Serrin (1972) persist in the zero-viscosity limit. Our analysis indicates that first there are no solutions with slip-discontinuity for the stationary, self-similar Euler equations, and second that the solutions of Navier–Stokes approach the single-cell solution of the Euler equations in the zero-viscosity limit. Numerical calculations indicate the presence of double-celled

solutions, but this happens for finite (even relatively large viscosities) and does not persist as the viscosity decreases.

We now provide an outline of the work. We introduce in (1.1) the self-similar transformation

$$\begin{aligned} u(r,z) &= \frac{1}{r}U(\xi), \quad v(r,z) = \frac{1}{r}V(\xi), \quad w(r,z) = \frac{1}{r}W(\xi), \\ p(r,z) &= \frac{1}{r^2}P(\xi), \quad \psi(r,z) = r\theta(\xi), \end{aligned} \tag{1.2}$$

motivated by the scale-invariance properties of Navier–Stokes equations, where $\xi = \frac{z}{r}$. In (1.2) we have used $\psi(r,z)$ the stream function

$$u = -\frac{1}{r}\frac{\partial \psi}{\partial z}, \quad w = \frac{1}{r}\frac{\partial \psi}{\partial r}$$

while $\theta(\xi)$ is its self-similar form connected to $(U, W)$ via

$$U = -\theta', \quad W = \theta - \xi\theta'. \tag{1.3}$$

This leads, for the axisymmetric Euler equations, to a system of ordinary differential equations for $(\theta, V, P)$

$$\left[\frac{\theta^2}{2} + (1+\xi^2)P\right]' = -\xi V^2, \tag{1.4a}$$

$$V'\theta = 0, \tag{1.4b}$$

$$\left[\theta^2 - \xi\left(\frac{\theta^2}{2}\right)' + P\right]' = 0, \tag{1.4c}$$

where $(U, W)$ are calculated via (1.3). The same transformation leads for the axisymmetric Navier–Stokes equations to the system

$$\left[\frac{\theta^2}{2} + (1+\xi^2)P\right]' = \nu\left[\xi\theta - (1+\xi^2)\theta'\right]' - \xi V^2, \tag{1.5a}$$

$$V'\theta = \nu\left[3\xi V' + (1+\xi^2)V''\right], \tag{1.5b}$$

$$\left[\theta^2 - \xi\left(\frac{\theta^2}{2}\right)' + P\right]' = \nu\left[\xi\theta - \xi^2\theta' - \xi(1+\xi^2)\theta''\right]', \tag{1.5c}$$

augmented with the physically relevant boundary conditions (see Sect. 2 for the derivations).

First, we consider (1.4). Imposing no-penetration conditions on the boundary and the vortex core we derive explicit solutions that correspond to either ascending or descending flows. To examine whether a double-celled vortex may occur for the Euler equations, we consider the existence of solutions with slip discontinuity in velocity. These would emerge from the Rankine-Hugoniot conditions for (1.4),

$$[\![P]\!] = 0, \qquad [\![\theta V]\!] = 0, \qquad [\![\theta\,\theta']\!] = 0, \tag{1.6}$$

where $[\![\cdot]\!]$ is the jump operator. We prove that there do not exist solutions of the self-similar Euler equations with discontinuities at a finite number of points that satisfy the jump conditions (1.6). This nonexistence result is then extended to a class of flows where there is mass input or loss through the vortex line. For the aforementioned flows, the explicit continuous solutions are also derived. The nonexistence result leads to conjecture that the double-celled vortices cannot persist in the limit as the viscosity goes to zero.

Next, we focus on the stationary self-similar axisymmetric Navier–Stokes system (1.5) in the context of a vortex core interacting with a boundary. This problem is reduced to a coupled integrodifferential system for $(\theta(\xi), V(\xi))$

$$\frac{\theta^2}{2} - \nu\Big[(1+\xi^2)\theta' + \xi\theta\Big] = \mathcal{G}(\xi), \tag{1.7a}$$

$$\nu(1+\xi^2)V'' + \Big(3\nu\xi - \theta\Big)V' = 0, \tag{1.7b}$$

with boundary conditions

$$\theta = \theta' = V = 0 \ \text{ at } \ \xi = 0, \qquad V \to V_\infty, \ U \to 0, \ \text{ as } \xi \to \infty. \tag{1.8}$$

where the functional $\mathcal{G}$ depending on $V(\cdot)$ and $\xi$ is defined via

$$\mathcal{G}(\xi) = \mathcal{G}(V(\cdot), \xi) = \xi\sqrt{1+\xi^2}\int_\xi^\infty \frac{1}{\zeta^2(1+\zeta^2)^{\frac{3}{2}}}\Big(\int_0^\zeta sV^2(s)\mathrm{d}s\Big)\mathrm{d}\zeta + E_0\phi(\xi), \tag{1.9}$$

and $\phi(\xi)$ is the function

$$\phi(\xi) := \xi\big(\sqrt{1+\xi^2} - \xi\big).$$

The system is recast into two equivalent integrodifferential formulations and provides a common framework encompassing the pioneering works on this problem of Goldshtik (1960), Serrin (1972) and Goldshtik and Shtern (1990). Existence of solutions for (1.7) is provided under the conditions described in Serrin (1972). Moreover the system (1.7) is solved numerically using an iterative solver and a numerical bifurcation diagram is presented, see Fig. 11.

We then focus on the zero-viscosity limit from Navier–Stokes to Euler in the self-similar stationary setting. This leads to study the zero-viscosity limit $\nu \to 0$ for the integrodifferential system (1.7). The problem is conveniently recasted as an autonomous system,

$$\begin{aligned} \nu\frac{\mathrm{d}\Theta_\nu}{\mathrm{d}x} &= \tfrac{1}{2}\Theta_\nu^2 - \mathcal{F}(V_\nu; x), \\ \nu\frac{\mathrm{d}^2V_\nu}{\mathrm{d}x^2} &= \Theta_\nu\frac{\mathrm{d}V_\nu}{\mathrm{d}x}, \end{aligned} \tag{1.10}$$

where $\mathcal{F}(V_\nu; x)$ is the analogue of (1.9) (defined in (5.17) see Sect. 5.2). An analysis of the possible configurations of solutions of (1.10) (based on ideas of Goldstick 1960) leads to a-priori estimates for solutions and classifying the potential shapes of the stream function to three configurations. To investigate the zero-viscosity limit, we employ compactness methods and exploit techniques developed in the theory of zero-viscosity limits for Riemann problems of conservation laws, Tzavaras (1996), Papadoperakis (1999). The sequence $\{V_\nu\}$ consists of monotone, uniformly bounded functions, and by Helly's theorem converges along subsequences to a limit $V$. The limit generates a Borel measure $dV$ which may be viewed as a limit of a family of probability measures capturing the averaging process as $\nu \to 0$. We pursue two theories: the first is based on $L^p$ estimates for the stream function and variation estimates for the velocity. It uses weak convergence methods and leads to the convergence Theorem 5.4. The latter is not fully satisfactory due to the weak bounds available for the stream function. In a second step, under more restrictive conditions on the data for the problem, we obtain uniform variation estimates and invoke Helly's theorem to conclude almost everywhere convergence (along subsequences) from the Navier–Stokes solutions to the Euler solutions. The convergence results are stated in Theorem 5.8, Proposition 5.9, and Corollary 5.10. They permit to characterize admissibility restrictions for the stationary Euler solutions emerging from Navier–Stokes in this setting.

Finally, we study the boundary layer in the case of a model problem for (1.10) that captures the essential behaviour of our system. We use methods of asymptotic analysis, namely inner and outer solutions and matched asymptotic expansions. We deduce that the boundary layer is of order $\nu^{2/3}$ and provide an asymptotic description of the stream function $\Theta_\nu$ (see (6.7)) and of $V_\nu$ (see (6.12)).

Along with previous works (Long 1958; Goldshtik 1960; Serrin 1972; Goldshtik and Shtern 1990) a complete picture emerges regarding self-similar stationary flows of the form (1.2) for the equations (1.1). These solutions capture the interaction of a line vortex with a solid boundary and the effects of secondary flows induced by such interaction; it provides a good description of the core of a swirling flow. As already noted in Long (1961), these solutions are singular at the origin. Attempts to resolve this issue are available in the Applied Mathematics literature, see "Appendix B" for an outline, but to the best of our knowledge a systematic mathematical understanding is presently lacking in a setting of axisymmetric flows. In addition, significant problems remain open: for example, it is well known that tornadoes are moving, while the self-similar *ansatz* provides a stationary structure. An important problem would be to obtain an *ansatz* for a swirling flow that is moving, or the (related) problem of determining the stability (or instability) of the self-similar steady flows. Additional effects like compressibility, buoyancy and variations in temperature are expected to play a role in tornadoes and are not taken into account in the simplified model of axisymmetric swirling flows. The reader is referred to the relatively recent excellent review (Rotunno 2013) for fluid-mechanics models of tornadoes.

The work is organized as follows: In Sect. 2, we introduce the self-similar ansatz and derive the systems (1.4) and (1.5) that are used in the rest of this work. Sections 3 and 4 are devoted to stationary self-similar axisymmetric Euler equations. In Sect. 3, an explicit continuous solution of (1.4) is derived, while in Sect. 4 we investigate the existence of discontinuous solutions with finite number of discontinuities. In Sect. 4,

Euler solutions are also studied for flows with input of mass through the vortex line. In Sect. 5, we study self-similar stationary solutions for axisymmetric Navier–Stokes. After presenting some of their properties, we examine their limiting behaviour as $\nu \to 0$ using compactness methods and analytical ideas from the theory of Borel measures. The results are stated in Theorems 5.4, 5.8 and Corollary 5.10. In Sect. 6, there is an asymptotic analysis of the boundary layer for a model problem, where inner and outer expansions lead to an explicit form of an asymptotic solution. In Sect. 7, a numerical scheme is presented for solving the stationary, self-similar system (1.10). We present indicative profiles of typical flows that appear for various values of the parameters and calculate a bifurcation of solutions in terms of the dimensionless parameters $(\frac{E_0}{V_\infty}, \frac{\nu}{V_\infty})$. The diagram is computed by solving the system (1.10) numerically and characterizing solutions according to the zone they belong, see Sects. 5.3 and 7.4.

In "Appendix A" we list Navier–Stokes in cylindrical coordinates. As our study is motivated from the study of tornadoes, we present for the convenience of the reader in "Appendix B" a quick review of models used in the literature for tornado modelling.

## 2 Preliminaries

We consider the equations of motion for an incompressible homogeneous viscous fluid, with constant density $\rho = 1$:

$$\vec{u}_t + (\vec{u} \cdot \nabla)\vec{u} = -\nabla p + \nu \, \Delta \vec{u}, \tag{2.1a}$$

$$\nabla \cdot \vec{u} = 0, \tag{2.1b}$$

where $\vec{u} : \mathbb{R}^3 \times \mathbb{R}_+ \to \mathbb{R}^3$ is the velocity vector of the fluid, $p : \mathbb{R}^3 \times \mathbb{R}_+ \to \mathbb{R}$ is the pressure, and $\nu \geq 0$ is the coefficient of kinematic viscosity. The first equation represents the conservation of momentum, while the second is the incompressibility condition and may be interpreted as describing conservation of mass. For $\nu > 0$, the system (2.1) is the so-called Navier–Stokes equations, while when viscosity effects are omitted, the corresponding system (2.1) with $\nu = 0$ is the (incompressible) Euler equations.

### 2.1 Axisymmetric Navier–Stokes Equations

In three space dimensions, introducing cylindrical coordinates $(r, \vartheta, z)$: $x_1 = r \cos\vartheta$, $x_2 = r \sin\vartheta$, $x_3 = z$, and the attached unit vector system

$$\vec{e}_r = (\cos\vartheta, \sin\vartheta, 0), \quad \vec{e}_\vartheta = (-\sin\vartheta, \cos\vartheta, 0), \quad \vec{e}_z = (0, 0, 1),$$

we express the velocity vector $\vec{u}$ in cylindrical coordinates as

$$\vec{u} = u(r, \vartheta, z, t)\vec{e}_r + v(r, \vartheta, z, t)\vec{e}_\vartheta + w(r, \vartheta, z, t)\vec{e}_z.$$

A flow is called axisymmetric if the velocity $\vec{u}$ does not depend on the azimuthal angle $\vartheta$, i.e.

$$\vec{u} = u(r, z, t)\vec{e}_r + v(r, z, t)\vec{e}_\vartheta + w(r, z, t)\vec{e}_z.$$

The velocity component $v$ in the direction of $\vec{e}_\vartheta$ is called the swirl velocity. If the swirl is everywhere equal to zero, i.e. $v \equiv 0$, we name such flows as flows without swirl. Otherwise we call them axisymmetric flows with swirl.

Using that the velocity $\vec{u}$ does not depend on $\vartheta$, we derive the axisymmetric Navier–Stokes equations which have the following form (see "Appendix A")

$$\frac{\partial u}{\partial t} + u\frac{\partial u}{\partial r} + w\frac{\partial u}{\partial z} - \frac{v^2}{r} = \nu\Big[\frac{1}{r}\frac{\partial}{\partial r}\Big(r\frac{\partial u}{\partial r}\Big) + \frac{\partial^2 u}{\partial z^2} - \frac{u}{r^2}\Big] - \frac{\partial p}{\partial r}, \tag{2.2a}$$

$$\frac{\partial v}{\partial t} + u\frac{\partial v}{\partial r} + w\frac{\partial v}{\partial z} + \frac{uv}{r} = \nu\Big[\frac{1}{r}\frac{\partial}{\partial r}\Big(r\frac{\partial v}{\partial r}\Big) + \frac{\partial^2 v}{\partial z^2} - \frac{v}{r^2}\Big], \tag{2.2b}$$

$$\frac{\partial w}{\partial t} + u\frac{\partial w}{\partial r} + w\frac{\partial w}{\partial z} = \nu\Big[\frac{1}{r}\frac{\partial}{\partial r}\Big(r\frac{\partial w}{\partial r}\Big) + \frac{\partial^2 w}{\partial z^2}\Big] - \frac{\partial p}{\partial z}, \tag{2.2c}$$

$$\frac{1}{r}\frac{\partial}{\partial r}(ru) + \frac{\partial w}{\partial z} = 0. \tag{2.2d}$$

For general axisymmetric flows, the vorticity vector $\vec{\omega} = \nabla \times \vec{u}$ is expressed as

$$\vec{\omega} = \big(\omega_r, \omega_\vartheta, \omega_z\big) = \Big( -\frac{\partial v}{\partial z}, \frac{\partial u}{\partial z} - \frac{\partial w}{\partial r}, \frac{1}{r}\frac{\partial}{\partial r}(rv)\Big),$$

where $\omega_\vartheta := \frac{\partial u}{\partial z} - \frac{\partial w}{\partial r}$ is the component of vorticity in the $\vec{e}_\vartheta$-direction. Note that for flows *without swirl* only the vorticity in the direction of $\vec{e}_\vartheta$ survives: $\vec{\omega} = \omega_\vartheta \vec{e}_\vartheta$.

The continuity equation (2.2d) may be integrated using the axisymmetric stream function $\psi(r, z, t)$ connected to $u$ and $w$ via

$$u = -\frac{1}{r}\frac{\partial \psi}{\partial z} \quad \text{and} \quad w = \frac{1}{r}\frac{\partial \psi}{\partial r}.$$

The stream function $\psi$ and the vorticity component $\omega_\vartheta$ are independent of the swirl velocity $v$; hence, an equivalent formulation of (2.2a)–(2.2d) is given by

$$\frac{\partial \omega_\vartheta}{\partial t} + u\frac{\partial \omega_\vartheta}{\partial r} + w\frac{\partial \omega_\vartheta}{\partial z} - \omega_\vartheta\frac{u}{r} = \nu\Big[\Delta\omega_\vartheta - \frac{\omega_\vartheta}{r^2}\Big] + \frac{\partial}{\partial z}\Big(\frac{v^2}{r}\Big), \tag{2.3a}$$

$$\frac{\partial v}{\partial t} + u\frac{\partial v}{\partial r} + w\frac{\partial v}{\partial z} + v\frac{u}{r} = \nu\Big[\Delta v - \frac{v}{r^2}\Big], \tag{2.3b}$$

$$\omega_\vartheta = -\frac{1}{r}\Delta\psi + \frac{2}{r^2}\frac{\partial \psi}{\partial r}, \tag{2.3c}$$

$$\big(u, w\big) = \frac{1}{r}\nabla^\perp \psi, \tag{2.3d}$$

in terms of $\omega_\theta$, $v$ and $\psi$, where

$$\Delta f = \frac{1}{r}\frac{\partial}{\partial r}\Big(r\frac{\partial f}{\partial r}\Big) + \frac{\partial^2 f}{\partial z^2} \qquad \text{and} \qquad \nabla^\perp f = \Big( -\frac{\partial f}{\partial z}, \frac{\partial f}{\partial r}\Big).$$

This formulation is equivalent with the three-dimensional Navier–Stokes equations, Majda and Bertozzi (2001).

### 2.2 Self-Similar Formulation

In the analysis of partial differential equations it is often beneficial to seek solutions that conform with symmetry properties of the problem, for instance invariance under rotations, dilations, etc. The invariance of the Navier–Stokes equations under the scaling

$$\vec{u}(t,r,z) = \lambda\,\vec{u}(\lambda^2 t, \lambda r, \lambda z) \quad \text{and} \quad p(t,r,z) = \lambda^2\, p(\lambda^2 t, \lambda r, \lambda z), \tag{2.4}$$

for $\lambda > 0$, suggests to look for self-similar solutions of (2.2a)–(2.2d) that follow the ansatz

$$\begin{aligned} u(t,r,z) &= \frac{1}{r}U(s,\xi), \quad v(t,r,z) = \frac{1}{r}V(s,\xi), \quad w(t,r,z) = \frac{1}{r}W(s,\xi), \\ p(t,r,z) &= \frac{1}{r^2}P(s,\xi), \quad \psi(t,r,z) = r\Psi(s,\xi), \quad \omega_\vartheta(t,r,z) = \frac{1}{r^2}\Omega(s,\xi), \end{aligned} \tag{2.5}$$

in the variables $\xi = \frac{z}{r}$ and $s = \frac{r}{\sqrt{t}}$. Such an ansatz induces a singularity at $r = 0$. In the literature related to tornadoes the singularity is considered to represent the line vortex resembling the tornado core, Morton (1966). Using the ansatz (2.5) in (2.2a)–(2.2d), a tedious but straightforward calculation yields the system of partial differential equations for $(U, V, W)$,

$$\begin{aligned} s\Big(U - \frac{s^2}{2}\Big)U_s + \big(W - \xi U\big)U_\xi - \big(U^2 + V^2\big) &= \nu\Big[\mathcal{H}U - U\Big] + 2P + \xi P_\xi - sP_s, \\ s\Big(U - \frac{s^2}{2}\Big)V_s + \big(W - \xi U\big)V_\xi &= \nu\Big[\mathcal{H}V - V\Big], \\ s\Big(U - \frac{s^2}{2}\Big)W_s + \big(W - \xi U\big)W_\xi - UW &= \nu\Big[\mathcal{H}W\Big] - P_\xi, \\ sU_s + W_\xi - \xi U_\xi &= 0, \end{aligned} \tag{2.6}$$

where the operator $\mathcal{H}$ is defined as

$$\mathcal{H}f = \Big[-\xi f + \big((1+\xi^2)f\big)_\xi\Big]_\xi - sf_s - 2s\xi f_{s\xi} + s^2 f_{ss}. \tag{2.7}$$

The same ansatz transforms the velocity-vorticity equations (2.3a)–(2.3d) into the form

$$\begin{aligned} s\Big(U - \frac{s^2}{2}\Big)\Omega_s + \big(W - \xi U\big)\Omega_\xi - 3U\Omega - 2VV_\xi &= \nu\big[\mathcal{D}\Omega - \Omega\big], \\ s\Big(U - \frac{s^2}{2}\Big)V_s + \big(W - \xi U\big)V_\xi &= \nu\big[\mathcal{H}V - V\big], \\ \Psi - \xi\Psi_\xi - s\Psi_s + 2s\xi\Psi_{s\xi} - s^2\Psi_{ss} - (1+\xi^2)\Psi_{\xi\xi} &= \Omega, \\ \Big(-\Psi_\xi, \Psi - \xi\Psi_\xi + s\Psi_s\Big) &= \big(U, W\big), \end{aligned} \tag{2.8}$$

where $\mathcal{H}$ is defined in (2.7) and $\mathcal{D}$ is given by

$$\mathcal{D}f = 4f + 5\xi f_\xi - 3sf_s - 2s\xi f_{s\xi} + s^2 f_{ss} + (1+\xi^2) f_{\xi\xi}. \tag{2.9}$$

The choice of ansatz is not unique and various self-similar transformations can be used for the Navier–Stokes equations, for instance, one may consider an ansatz in variables $\xi = \frac{z}{r}$ and $\tau = \frac{t}{r^2}$.

### 2.3 Stationary Self-Similar Formulation

The tornadic funnel typically moves slowly compared to the internal swirling velocities, Rotunno (2013). This motivates to represent the core of the tornado via a vortex singularity, following (Long 1958; Goldshtik 1960), and to study stationary axisymmetric self-similar solutions for the Navier–Stokes equations. Letting $\xi = \frac{z}{r}$, we seek self-similar stationary solutions of (2.2a)–(2.2d) in the form

$$\begin{aligned} u(r,z) &= \frac{1}{r}U(\xi), \quad v(r,z) = \frac{1}{r}V(\xi), \quad w(r,z) = \frac{1}{r}W(\xi), \\ p(r,z) &= \frac{1}{r^2}P(\xi), \quad \psi(r,z) = r\Psi(\xi), \quad \omega_\vartheta(r,z) = \frac{1}{r^2}\Omega(\xi). \end{aligned} \tag{2.10}$$

Such solutions satisfy the system of ordinary differential equations

$$-U\Big(\xi U\Big)' + U'W - V^2 = \nu\Big[\mathcal{L}U - U\Big] + 2P + \xi P', \tag{2.11a}$$

$$-U\Big(\xi V\Big)' + V'W + UV = \nu\Big[\mathcal{L}V - V\Big], \tag{2.11b}$$

$$-U\Big(\xi W\Big)' + W'W = \nu\mathcal{L}W - P', \tag{2.11c}$$

$$W' - \xi U' = 0 \tag{2.11d}$$

where $\xi \in \mathbb{R}_+$ and the operator $\mathcal{L}$ defined as

$$\mathcal{L}f = \Big[ -\xi f + \Big((1+\xi^2)f\Big)'\Big]'. \tag{2.12}$$

If we multiply (2.11a) by $\xi$ and subtract it from (2.11c), we can rewrite the system as

$$\begin{aligned} \Big[\frac{1}{2}\Big(W - \xi U\Big)^2 + (1+\xi^2)P\Big]' &= \nu\big\{\mathcal{L}W - \xi\mathcal{L}U + \xi U\big\} - \xi V^2, \\ V'\Big(W - \xi U\Big) &= \nu\big\{\mathcal{L}V - V\big\}, \\ \Big[W\Big(W - \xi U\Big) + P\Big]' &= \nu\mathcal{L}W, \\ \Big(W - \xi U\Big)' &= -U. \end{aligned}$$

For convenience, we introduce $\theta = W - \xi U$. One checks from (2.3d) and (2.10) that $\theta(\xi) = \Psi(\xi)$ is the self-similar version of the stream function and

$$\theta = W - \xi U, \quad U = -\theta', \quad W = \theta - \xi\theta'. \tag{2.13}$$

A tedious but straightforward computation renders (2.3) to a nonlinear system of ordinary differential equations for $(\theta, V, P)$,

$$\left[\frac{\theta^2}{2} + (1+\xi^2)P\right]' = \nu\left[\xi\theta - (1+\xi^2)\theta'\right]' - \xi V^2, \tag{2.14a}$$

$$V'\theta = \nu\left[3\xi V' + (1+\xi^2)V''\right], \tag{2.14b}$$

$$\left[\theta^2 - \xi\left(\frac{\theta^2}{2}\right)' + P\right]' = \nu\left[\xi\theta - \xi^2\theta' - \xi(1+\xi^2)\theta''\right]', \tag{2.14c}$$

where the viscosity $\nu$ is a parameter and $(U, W)$ are determined by (2.13). The aim is to study (2.14) in both the viscous $\nu > 0$ as well as the inviscid $\nu = 0$ cases and to investigate the limiting relationship. Sections 3 and 4 are devoted to the inviscid case $\nu = 0$: In Sect. 3 an explicit solution for (2.14) (with $\nu = 0$) is obtained. The existence of solutions with slip discontinuities is examined in Sect. 4. In Sect. 5, we express the system (2.14) for $\nu > 0$ into an equivalent integrodifferential formulation and study its limit as $\nu \to 0$. Numerical solutions are illustrated in Sect. 7.

## 3 A Stationary Self-Similar Solution for the Axisymmetric Euler Equations

Consider first the Euler equations (2.14) with $\nu = 0$:

$$\left[\frac{\theta^2}{2} + (1+\xi^2)P\right]' = -\xi V^2\,, \tag{3.1a}$$

$$V'\theta = 0\,, \tag{3.1b}$$

$$\left[\theta^2 - \xi\left(\frac{\theta^2}{2}\right)' + P\right]' = 0\,, \tag{3.1c}$$

$$\theta' = -U. \tag{3.1d}$$

Equation (3.1b) implies that if $\theta(\xi) \neq 0$ then $V(\xi)$ is a constant function. So, assume first that $\theta \neq 0$ for $\xi \in (0, \infty)$ and that

$$V \equiv V_0, \tag{3.2}$$

where $V_0$ is a constant proportional to the circulation around the axis. (The case where $\theta$ vanishes and where $V$ may exhibit discontinuities is examined in the next section.) Substituting (3.2) yields

$$\xi(1+\xi^2)\Big(\frac{\theta^2}{2}\Big)' - (1+2\xi^2)\Big(\frac{\theta^2}{2}\Big) = -\frac{\xi^2}{2}{V_0}^2 - E_0(1+\xi^2) + A_0\,, \tag{3.3a}$$

$$P = \xi\Big(\frac{\theta^2}{2}\Big)' - \theta^2 + E_0\,, \tag{3.3b}$$

where $E_0$ and $A_0$ are integration constants. Dividing equation (3.3a) by $\xi^2(1+\xi^2)^{\frac{3}{2}}$ gives

$$\left[\frac{1}{\xi\sqrt{1+\xi^2}}\frac{\theta^2}{2}\right]' = -\frac{{V_0}^2}{2}\left[\frac{\xi}{\sqrt{1+\xi^2}}\right]' + E_0\left[\frac{\sqrt{1+\xi^2}}{\xi}\right]' - A_0\left[\frac{1+2\xi^2}{\xi\sqrt{1+\xi^2}}\right]'.$$

After an integration, we eventually obtain an explicit form for the stream function $\theta$ and an explicit solution for the Euler system (3.1a)–(3.1d)

$$\frac{\theta^2}{2} = -\Big(\frac{V_0^2}{2} + 2A_0 - E_0\Big)\xi^2 + k_0\xi\sqrt{1+\xi^2} + \Big(E_0 - A_0\Big)\,, \tag{3.4a}$$

$$U = \frac{1}{\theta}\left[2\Big(\frac{V_0^2}{2} + 2A_0 - E_0\Big)\xi - k_0\frac{1+2\xi^2}{\sqrt{1+\xi^2}}\right], \tag{3.4b}$$

$$W = \frac{1}{\theta}\left[k_0\frac{\xi}{\sqrt{1+\xi^2}} + 2\Big(E_0 - A_0\Big)\right], \tag{3.4c}$$

$$P = -k_0\frac{\xi}{\sqrt{1+\xi^2}} + 2A_0 - E_0\,, \tag{3.4d}$$

where $V(\xi)$ is given by (3.2) and $E_0$, $A_0$ and $k_0$ are integration constants.

We supplement system (3.1a)–(3.1d) with suitable boundary conditions. Recall that our objective is to model a vortex line that interacts with a boundary surface. We impose no-penetration boundary condition at the boundary, namely $w = 0$ at $z = 0$. Moreover, we assume that $u = 0$ as $r \to 0$ which ensures that no mass is added or lost through the vortex line. Expressing these conditions in terms of the self-similar functions (2.10) leads to

$$W(0) = 0 \quad \text{and} \quad U(\xi) \to 0 \quad \text{as} \quad \xi \to \infty, \tag{3.5}$$

or in terms of $\theta$

$$\theta(0) = 0 \quad \text{and} \quad \theta'(\xi) \to 0 \quad \text{as} \quad \xi \to \infty. \tag{3.6}$$

The boundary conditions applied to (3.4) provide the relations

$$E_0 = A_0\,, \tag{3.7a}$$

$$k_0 = \frac{{V_0}^2}{2} + E_0. \tag{3.7b}$$

The derivation of (3.7a) is direct. To derive relation (3.7b), note that (3.4a), (3.4b) imply

$$U = \frac{1}{\theta}\left[2\Big(\frac{V_0^2}{2} + E_0\Big)\xi - k_0\frac{1+2\xi^2}{\sqrt{1+\xi^2}}\right] = \frac{2\Big(\frac{V_0^2}{2} + E_0\Big) - k_0\frac{1+2\xi^2}{\xi\sqrt{1+\xi^2}}}{\pm\sqrt{-2\Big(\frac{V_0^2}{2} + E_0\Big) + 2k_0\frac{\sqrt{1+\xi^2}}{\xi}}}$$

$$\xrightarrow{\xi\to\infty} \mp\sqrt{-2\Big(\frac{V_0^2}{2} + E_0\Big) + 2k_0}$$

Thus, as $\xi \to \infty$

$$U(\infty) = 0 = \mp\sqrt{-2\Big(\frac{V_0^2}{2} + E_0\Big) + 2k_0}\,,$$

which in turn implies (3.7b).

Substituting (3.7a)–(3.7b) into (3.4), we obtain the explicit formula

$$\theta^2 = 2k_0\,\phi(\xi), \tag{3.8}$$

with $\phi$ the function

$$\phi(\xi) := \xi\big(\sqrt{1+\xi^2} - \xi\big). \tag{3.9}$$

**Lemma 3.1** (Properties of $\phi(\xi)$). *The function $\phi(\xi)$ in (3.9) is shown in Fig. 1 and has the properties:*

1. *$\phi(\xi)$ is non-negative and bounded, $0 < \phi(\xi) < \frac{1}{2}$ for $0 < \xi < \infty$.*
2. *$\phi(0) = 0$ and $\lim_{\xi\to\infty}\phi(\xi) = \frac{1}{2}$.*
3. *$\phi(\xi)$ is increasing and concave with*

$$\phi'(\xi) = \frac{1}{\sqrt{1+\xi^2}}\big(1 - 2\phi(\xi)\big) > 0, \quad \phi''(\xi) = -\frac{1-2\phi(\xi)}{(1+\xi^2)^{\frac{3}{2}}}\big(\xi + 2\sqrt{1+\xi^2}\big) < 0.$$

The sign of $\phi$ provides a constraint on the existence of $\theta$. From (3.8), $\theta(\xi)$ is well-defined iff $k_0 = E_0 + \frac{V_0^2}{2} > 0$. Under this restriction, we derive an explicit family of solutions depending on two parameters $V_0$, $E_0$

$$\theta = \pm\sqrt{2k_0\phi(\xi)}, \qquad U = \mp\sqrt{\frac{k_0}{2\phi(\xi)}}\left[\frac{1-2\phi(\xi)}{\sqrt{1+\xi^2}}\right], \qquad V = V_0,$$
$$W = \pm\sqrt{\frac{k_0}{2\phi(\xi)}}\frac{\xi}{\sqrt{1+\xi^2}}, \qquad P = \left(k_0 - \frac{V_0^2}{2}\right) - k_0\frac{\xi}{\sqrt{1+\xi^2}}. \tag{3.10}$$

**Fig. 1** Functions $\phi(\xi)$ and $\phi'(\xi)$

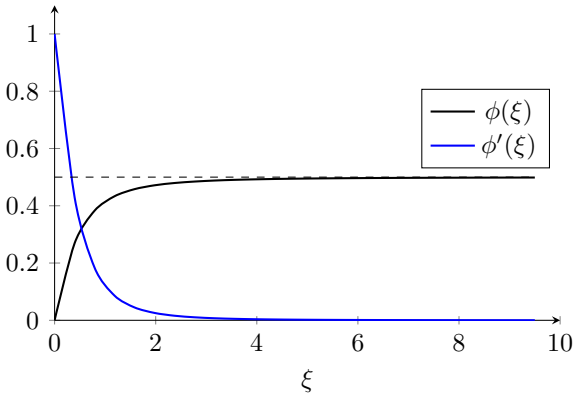


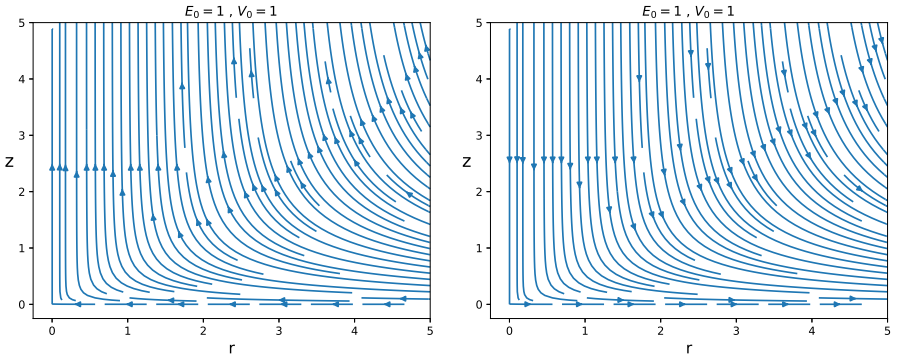


(a) $\theta > 0$ (b) $\theta < 0$

**Fig. 2** Velocity vector field $(u, w)$ in $(r, z)$ plane

Observe that $\theta(\xi)$ can be either positive or negative. If $\theta$ is positive, then the flow is directed inwards near the plane $z = 0$ and upwards near the vortex line. Conversely, if $\theta$ is negative, the flow is directed outwards near the plane $z = 0$ and downwards near the vortex line. In Fig. 2, two vector fields of $(u, w)$, see (3.11), are depicted, corresponding to the updraft and downdraft flows, depending on the sign of the streamfunction $\theta$.

Note that $P(\xi = 0) = E_0$ and $P(\xi = \infty) = -\frac{V_0^2}{2}$ and, as $P(\xi)$ is decreasing, the values of $P$ range from $-\frac{V_0^2}{2}$ to $E_0$. The constraint $k_0 > 0$ may be interpreted as

$$k_0 = E_0 + \frac{V_0^2}{2} = P(\xi = 0) - P(\xi = \infty) > 0.$$

As $p = \frac{P}{r^2}$ and $v = \frac{V}{r}$ the constraint may be thought as presenting a difference between pressure-induced forces at the top of the vortex core and the intersection of the vortex core with the boundary. $V_0$ is a measure of the circulation around the vortex core.

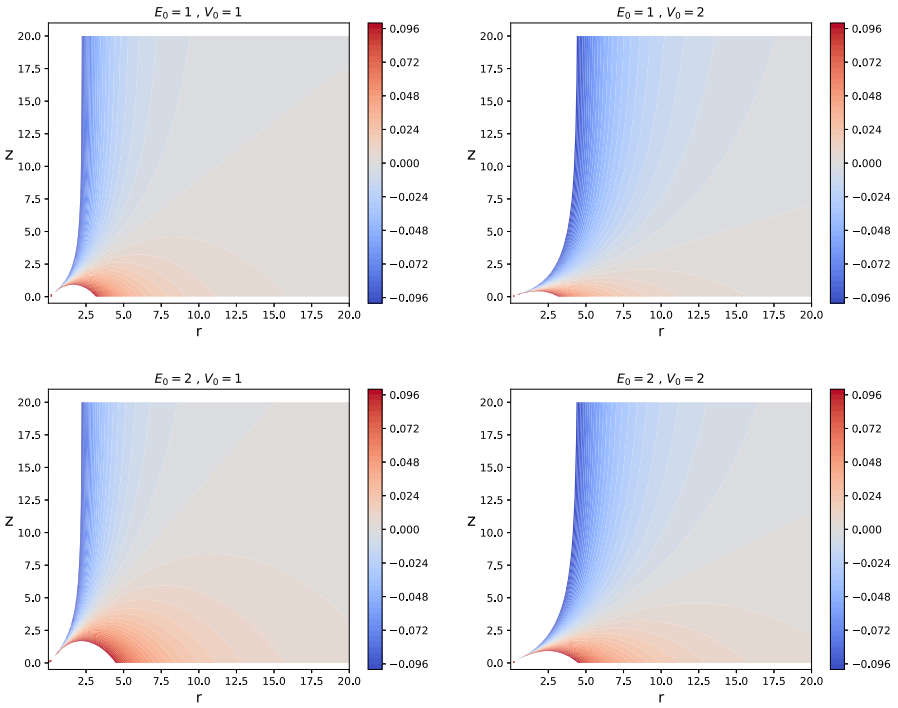


**Fig. 3** Contour plots of pressure $p$ in $(r, z)$ plane for $V_0 = 1, 2$ and $E_0 = 1, 2$

Returning to the original variables through (2.10) we obtain

$$
\begin{aligned}
u(r,z) &= \mp\sqrt{\frac{k_0}{2}}\,\frac{(\sqrt{r^2+z^2}-z)^2}{r\sqrt{z(r^2+z^2)(\sqrt{r^2+z^2}-z)}}, \qquad v(r,z) = \frac{V_0}{r},\\
w(r,z) &= \pm\sqrt{\frac{k_0}{2}}\,\frac{z}{\sqrt{z(r^2+z^2)(\sqrt{r^2+z^2}-z)}},\\
p(r,z) &= \frac{1}{r^2}\Big(\big(k_0-\frac{V_0^2}{2}\big)-k_0\frac{z}{\sqrt{r^2+z^2}}\Big).
\end{aligned}
\tag{3.11}
$$

The streamlines of the vector field $(u, w)$ are sketched in Fig. 2, showing the two type of flows. In Fig. 3 contour plots of the pressure are shown for four different choices of the parameters $E_0$, $V_0$. The form of pressure field around $(r, z) = (0, 0)$ can be explained by examining its asymptotic behaviour around the origin. From (3.11) we have that

$$
p(r,z) = \frac{1}{r^2}\Big(E_0 - k_0\frac{z}{\sqrt{r^2+z^2}}\Big), \quad k_0 = E_0 + \frac{V_0^2}{2}
$$

Then, along the bottom($z = 0$) and vertical ($r = 0$) boundaries, $p(r, z)$ has the following asymptotic behaviour

$$\text{Bottom boundary:} \quad p(r,z) = \frac{E_0}{r^2} - \frac{k_0}{r^3} z + O(z^3), \quad z \to 0$$

$$\text{Vertical boundary:} \quad p(r,z) = \frac{k_0}{2z^2} - \frac{V_0^2}{2r^2} - \frac{3k_0}{8z^4} r^2 + O(r^4), \quad r \to 0$$

Values for the pressure are only presented with the same colour codes for the four plots in Fig. 3; what is outside the scale appears as white.

## 4 Do the Axisymmetric Euler Equations Admit Self-Similar Discontinuous Solutions?

We consider the Euler equations (3.1a)–(3.1d) and focus on solutions where $\theta$ vanishes and $V$ exhibits discontinuities. We study weak solutions for the system (3.1a)–(3.1d) and investigate the existence of discontinuous solutions subject to the boundary conditions used before.

### 4.1 Discontinuous Solutions—Weak Formulation

Let $\varphi \in C_c^\infty((0,\infty))$. Multiplying the equations (3.1a)–(3.1d) by $\varphi$ and integrating by parts, we obtain

$$-\int_0^\infty \left(\frac{\theta^2}{2} + (1+\xi^2)P\right)\varphi'(\xi)\mathrm{d}\xi = -\int_0^\infty \xi V^2(\xi)\varphi(\xi)\mathrm{d}\xi, \tag{4.1a}$$

$$-\int_0^\infty \Big(\theta(\xi)V(\xi)\Big)\varphi'(\xi)\mathrm{d}\xi = -\int_0^\infty U(\xi)V(\xi)\varphi(\xi)\mathrm{d}\xi, \tag{4.1b}$$

$$-\int_0^\infty \left(\theta^2 - \xi\Big(\frac{\theta^2}{2}\Big)' + P\right)\varphi'(\xi)\mathrm{d}\xi = 0, \tag{4.1c}$$

$$-\int_0^\infty \theta\varphi'(\xi)\mathrm{d}\xi = -\int_0^\infty U(\xi)\varphi(\xi)\mathrm{d}\xi. \tag{4.1d}$$

**Definition 4.1** The function $(\theta, V, P)$ of class $\theta \in W^{1,1}((0,\infty))$, $V, P \in BV((0,\infty)) \cap L^\infty((0,\infty))$ is a weak solution of the system (3.1a)–(3.1d) if (4.1) holds for any $\varphi \in C_c^\infty((0,\infty))$.

In the definition 4.1, $BV$ denotes the space of functions of bounded variation. This property ensures that right and left limits of $(\theta, V, P)$ exist at any point $\xi$. Since $\theta$ belongs to $W^{1,1}((0,\infty))$, then $\theta$ is absolutely continuous and of bounded variation. The derivative of $\theta$, i.e. $\theta' = -U$, exists almost everywhere and is Lebesgue integrable on $(0,\infty)$.

Suppose $(\theta, V, P)$ is a weak solution of (3.1a)–(3.1d). Using the theory of Sobolev spaces, Brezis (2010), Folland (2013), one may explore properties of system (4.1).

Recalling that $\theta$ and as a consequence $\theta^2$ are absolutely continuous, we get that $\theta^2 + \xi\left(\frac{\theta^2}{2}\right)' \in L^1_{loc}((0,\infty))$. Also, $P \in L^\infty((0,\infty)) \subset L^1_{loc}((0,\infty))$. Then, using (Brezis 2010, Lemma 8.1), (4.1c) implies there exists a constant $A$ such that

$$\theta^2 - \xi\left(\frac{\theta^2}{2}\right)' + P = A, \tag{4.2}$$

almost everywhere (a.e). The same lemma applied to (4.1a), (4.1b) and (4.1d) as follows. Using (Brezis 2010, Lemma 8.2) we rewrite (4.1a), (4.1b) and (4.1d) in the form

$$-\int_0^\infty \left(\frac{\theta^2}{2} + (1+\xi^2)P + \int_0^\xi \zeta V^2(\zeta)\mathrm{d}\zeta\right)\varphi'(\xi)\mathrm{d}\xi = 0. \tag{4.3a}$$

$$-\int_0^\infty \left(\theta(\xi)V(\xi) + \int_0^\xi U(\zeta)V(\zeta)\mathrm{d}\zeta\right)\varphi'(\xi)\mathrm{d}\xi = 0. \tag{4.3b}$$

$$-\int_0^\infty \left(\theta + \int_0^\xi U(\zeta)\mathrm{d}\zeta\right)\varphi'(\xi)d\xi = 0\,, \tag{4.3c}$$

where $\varphi \in C_c^\infty\big((0,\infty)\big)$. The integrals $\int_0^\xi \zeta V^2(\zeta)\mathrm{d}\zeta$, $\int_0^\xi U(\zeta)V(\zeta)\mathrm{d}\zeta$ and $\int_0^\xi U(\zeta)\mathrm{d}\zeta$ for $U = -\theta' \in L^1$ are well-defined. Using (Brezis 2010, Lemma 8.1), there are constants $B$, $C$ and $D$ such that

$$\frac{\theta^2}{2} + (1+\xi^2)P + \int_0^\xi \zeta V^2(\zeta)\mathrm{d}\zeta = B \quad \text{a.e.}, \tag{4.4a}$$

$$\theta(\xi)V(\xi) + \int_0^\xi U(\zeta)V(\zeta)\mathrm{d}\zeta = C \quad \text{a.e.}, \tag{4.4b}$$

$$\theta(\xi) + \int_0^\xi U(\zeta)\mathrm{d}\zeta = D \quad \text{a.e..} \tag{4.4c}$$

Letting $\xi \to a_-$ and $\xi \to b_+$ for $0 < a < b < \infty$ in (4.2) we obtain

$$\left(\theta^2 - \xi\left(\frac{\theta^2}{2}\right)' + P\right)\Big|_{\xi=a-}^{\xi=b_+} = 0.$$

This is combined with similar limits in (4.4a)–(4.4c) to conclude that $(\theta, V, P)$ a weak solution of (3.1a)–(3.1c) satisfies for $a < b$

$$\left(\frac{\theta^2(\xi)}{2} + (1+\xi^2)P(\xi)\right)\Big|_{a-}^{b_+} = -\int_a^b \zeta V^2(\zeta)\mathrm{d}\zeta, \tag{4.5a}$$

$$\left(\theta(\xi)V(\xi)\right)\Big|_{a-}^{b_+} = -\int_a^b U(\xi)V(\xi)\mathrm{d}\xi, \tag{4.5b}$$

$$\left(\theta^2 - \xi\left(\frac{\theta^2}{2}\right)' + P(\xi)\right)\Big|_{a-}^{b+} = 0, \tag{4.5c}$$

$$\theta(\xi)\Big|_{a-}^{b+} = -\int_a^b U(\xi)\mathrm{d}\xi, \tag{4.5d}$$

**Jump Discontinuities**

Let $(\theta, V, P)$ be a weak solution of (3.1a)–(3.1d) defined by Definition 4.1. Utilizing (4.5), we will compute the Rankine-Hugoniot jump conditions associated with the system. Suppose there exists a discontinuity at some point $\xi = \sigma, 0 < \sigma < \infty$ as in Fig. 4. Letting $a, b \to \sigma$, (4.5) reduces to

$$\frac{1}{2}\left(\theta_+^2 - \theta_-^2\right) + (1+\sigma^2)\left(P_+ - P_-\right) = 0, \tag{4.6a}$$

$$\theta_+ V_+ - \theta_- V_- = 0, \tag{4.6b}$$

$$\left(\theta_+^2 - \sigma\left(\frac{\theta_+^2}{2}\right)' - \left(\theta_-^2 - \sigma\left(\frac{\theta_-^2}{2}\right)'\right)\right) + \left(P_+ - P_-\right) = 0, \tag{4.6c}$$

$$\theta_+ - \theta_- = 0, \tag{4.6d}$$

where $\theta_\pm = \theta(\sigma\pm)$, $V_\pm = V(\sigma\pm)$ and $P_\pm = P(\sigma\pm)$ denote the one-sided limits at $\xi = \sigma$. Note that all one-sided limits exist and are finite since $(\theta, V, P)$ are of bounded variation.

The last equation in (4.6) implies that $\theta$ must be continuous for any $\xi \in (0, \infty)$, that is to say

$$\theta_- = \theta_+,$$

and thus, (4.6a)–(4.6c) provide the Rankine-Hugoniot jump conditions

$$[\![P]\!] = 0, \tag{4.7a}$$

$$[\![\theta V]\!] = 0, \tag{4.7b}$$

$$[\![\theta\,\theta']\!] = 0, \tag{4.7c}$$

where $[\![F]\!] = F_+ - F_-$ is the jump operator. It is easy to see that $P(\xi)$ must also be continuous for any $\xi \in (0, \infty)$. On the other hand, for $\theta(\sigma) = 0$ (4.7) implies that $V(\xi)$ and $\theta'(\xi)$ have a jump discontinuity at $\xi = \sigma$. (The case where $\theta(\sigma) \neq 0$ implies that $V$ is continuous and leads to solutions described in Section 3.)

### 4.1.1 Nonexistence of Discontinuous Solutions

Consider $(\theta, V, P)$ a weak solution of (3.1a)–(3.1c) given by definition (4.1) with a discontinuity at a fixed point $\xi = \sigma, \sigma \in (0, \infty)$. Recall that $\theta'$ and $V$ may exhibit

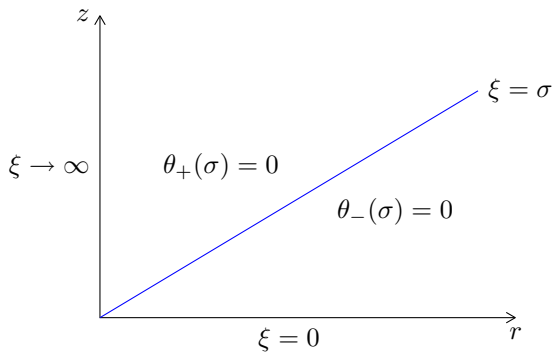


**Fig. 4** Domain of solutions with discontinuity

discontinuities, it suggests looking for solutions in the form

$$\theta(\xi) = \begin{cases} \theta_-(\xi), \\ \theta_+(\xi) \end{cases} \quad \text{and} \quad V(\xi) = \begin{cases} V_-(\xi), & \xi \in (0, \sigma) \\ V_+(\xi), & \xi \in (\sigma, \infty) \end{cases}$$

We solve the system (3.1a)–(3.1c) on $(0, \sigma)$ and $(\sigma, \infty)$ independently. Similar calculations to those described in Sect. 3 lead again to a solution $\theta$ in form (3.4a) on each domain. Note that $V(\xi)$ is again a constant function with $V_-$ and $V_+$ constants. Since discontinuous solutions occur when $\theta(\sigma) = 0$, the relation for $\theta$ becomes

$$\frac{\theta_\pm^2}{2} = k_\pm\Big(\phi(\xi) - \phi(\sigma)\Big) + \Big(k_\pm - \frac{V_\pm^2}{2} - 2A_\pm + E_\pm\Big)\big(\xi^2 - \sigma^2\big). \tag{4.8}$$

where $k_\pm$, $A_\pm$ and $E_\pm$ are integration constants. We next impose the boundary conditions (3.6), that is

$$\theta_-(0) = 0 \quad \text{and} \quad \theta_+'(\xi) \to 0 \quad \text{as} \quad \xi \to \infty,$$

which imply

$$k_- - \frac{V_-^2}{2} - 2A_- + E_- = -k_- \frac{1}{\sigma^2}\phi(\sigma), \tag{4.9}$$

$$k_+ - \frac{{V_+}^2}{2} - 2A_+ + E_+ = 0. \tag{4.10}$$

The derivation of (4.9) is direct. To derive relation (4.10), observe that (4.8) yields

$$\theta_+' = \frac{1}{\theta}\left[k_+\phi'(\xi) + 2\Big(k_+ - \frac{V_+^2}{2} - 2A_+ + E_+\Big)\xi\right]$$

$$= \frac{k_+\frac{\phi'(\xi)}{\xi} + 2\left(k_+ - \frac{V_+^2}{2} - 2A_+ + E_+\right)}{\pm\sqrt{2k_+\frac{\phi(\xi)-\phi(\sigma)}{\xi^2} + 2\left(k_+ - \frac{V_+^2}{2} - 2A_+ + E_+\right)\frac{\xi^2-\sigma^2}{\xi^2}}}$$
$$\xrightarrow{\xi\to\infty} \pm\sqrt{2\left(k_+ - \frac{V_+^2}{2} - 2A_+ + E_+\right)},$$

Therefore, as $\xi \to \infty$

$$\theta'(\infty) = 0 = k_+ - \frac{{V_+}^2}{2} - 2A_+ + E_+,$$

provides (4.10). Substituting now (4.9)–(4.10) into (4.8), we obtain the explicit formula

$$\frac{\theta^2}{2}(\xi) = \begin{cases} k_-\left[\phi(\xi) - \phi(\sigma) - \dfrac{\xi^2-\sigma^2}{\sigma^2}\phi(\sigma)\right], & \xi \in (0,\sigma) \\ k_+\left[\phi(\xi) - \phi(\sigma)\right], & \xi \in (\sigma,\infty) \end{cases} \tag{4.11}$$

From (3.4) and (4.11), we then derive an explicit family of discontinuous solutions depending on parameters $V_\pm$, $E_\pm$ and $\sigma$

$$U = \begin{cases} \dfrac{k_-}{\theta_-}\left[\dfrac{2\phi(\sigma)}{\sigma^2}\xi - \phi'(\xi)\right] \\ -\dfrac{k_+}{\theta_+}\,\phi'(\xi) \end{cases} \qquad W = \begin{cases} \dfrac{k_-}{\theta_-}\dfrac{\xi}{\sqrt{1+\xi^2}}, & \xi \in (0,\sigma) \\ \dfrac{k_+}{\theta_+}\left[\dfrac{\xi}{\sqrt{1+\xi^2}} - 2\phi(\sigma)\right], & \xi \in (\sigma,\infty) \end{cases} \tag{4.12a}$$

$$V = \begin{cases} V_- \\ V_+ \end{cases} \qquad P = \begin{cases} E_- - k_-\dfrac{\xi}{\sqrt{1+\xi^2}}, & \xi \in (0,\sigma) \\ E_+ - k_+\left(\dfrac{\xi}{\sqrt{1+\xi^2}} - 2\phi(\sigma)\right), & \xi \in (\sigma,\infty) \end{cases} \tag{4.12b}$$

where $E_- = k_-\left(1 + \frac{\phi(\sigma)}{\sigma^2}\right) - \frac{V_-^2}{2}$ and $E_+ = k_+(1 - 2\phi(\sigma)) - \frac{V_+^2}{2}$. Although solutions $U(\xi)$ and $W(\xi)$ tend to infinity near the discontinuity at $\xi = \sigma$, they achieve the required regularity in definition (4.1). In particular, examining the denominator yields

$$U(\xi) \sim W(\xi) \sim \begin{cases} \dfrac{k_-}{\theta_-} \sim \sqrt{\dfrac{k_-}{\Big(\phi(\xi)-\phi(\sigma)\Big)-\frac{\phi(\sigma)}{\sigma^2}\Big(\xi^2-\sigma^2\Big)}} \sim \dfrac{\sqrt{k_-}}{\sqrt{|\xi-\sigma|}}, & \text{as} \quad \xi \to \sigma_- \\ \dfrac{k_+}{\theta_+} \sim \sqrt{\dfrac{k_+}{\Big(\phi(\xi)-\phi(\sigma)\Big)}} \sim \dfrac{\sqrt{k_+}}{\sqrt{|\xi-\sigma|}}, & \text{as} \quad \xi \to \sigma_+ \end{cases}$$

and therefore the singularities $\xi = \sigma$ are integrable, i.e. $U, W \in L^1_{loc}((0,\infty))$. Analysis of these singularities leads to the following theorem.

**Theorem 4.2** *Let $(\theta, V, P)$ be a weak solution of (3.1a)–(3.1c) of class $\theta \in W^{1,1}((0,\infty))$, $V, P \in BV((0,\infty)) \cap L^\infty((0,\infty))$ which satisfies the boundary conditions*

$$V(0+) = V_0, \quad P(0+) = E_0, \quad \theta(0) = 0, \quad \theta'(\infty) = 0.$$

*There does not exist a solution $(\theta, V, P)$ with a discontinuity at a single point that fulfils jump conditions (4.7).*

***Proof*** Suppose there exists a weak solution $\theta$ given by (4.11) that satisfies jump conditions (4.7). Consider the condition (4.7c) applied to (4.11), namely

$$\theta_+(\sigma)\theta'_+(\sigma) = \theta_-(\sigma)\theta'_-(\sigma).$$

It provides a constraint on the constants $k_+, k_-$

$$\frac{k_+}{k_-} = 1 - 2\frac{\phi(\sigma)}{\sigma\,\phi'(\sigma)} < 0, \tag{4.13}$$

which implies that $k_+$ and $k_-$ must have different signs. The derivation of (4.13) is direct.

Next, we determine the signs of $k_+, k_-$. Since $\theta^2(\xi) > 0$ for $\xi \neq \sigma$, relation (4.11) imposes restrictions on the signs of $k_+, k_-$. Recall Lemma (3.1), the relation (4.11) implies that $k_+ > 0$. To find the sign of $k_-$, set

$$J(\xi) = \phi(\xi) - \phi(\sigma) - \frac{\phi(\sigma)}{\sigma^2}(\xi^2 - \sigma^2), \tag{4.14}$$

for $\xi \in (0,\sigma)$ and observe that $J(0) = J(\sigma) = 0$ and $J'' < 0$. Hence $J(\xi) > 0$ for $\xi \in (0,\sigma)$ and $k_- > 0$. This contradicts with (4.13), and thus, there does not exist a discontinuous solution $(\theta, V, P)$ that fulfils the jump conditions (4.7). □

### 4.1.2 Nonexistence of Multiple Discontinuities

Let $(\theta, V, P)$ be a weak solution of (3.1a)–(3.1d) with discontinuities at multiple points $\xi = \sigma_i$, $0 < \sigma_i < \infty$, $i > 0$. We consider first the case where the solution exhibits

discontinuities at two points $\sigma_1$ and $\sigma_2$, $\sigma_1 < \sigma_2$. This suggests seeking solutions in the form

$$\theta(\xi) = \begin{cases} \theta_1(\xi) \\ \theta_2(\xi) \\ \theta_3(\xi) \end{cases} \quad \text{and} \quad V(\xi) = \begin{cases} V_1(\xi), & \xi \in (0, \sigma_1) \\ V_2(\xi), & \xi \in (\sigma_1, \sigma_2) \\ V_3(\xi), & \xi \in (\sigma_2, \infty) \end{cases}.$$

To examine whether such solutions exist, it is sufficient to derive the solution $\theta$ by solving system (3.1a)–(3.1c) on each domain independently. Same calculations as those described in Sect. 3 lead to functions $\theta_1$, $\theta_2$ and $\theta_3$ of the form (3.4a), that is

$$\frac{\theta_j^2}{2} = k_j\phi(\xi) + \Big(k_j - \frac{V_j^2}{2} - 2A_j + E_j\Big)\xi^2 + \Big(E_j - A_j\Big), \quad j = 1, 2, 3 \tag{4.15}$$

where $A_j$, $E_j$, $k_j$ are integration constants. Note that $V(\xi)$ is again a constant function with $V_1$, $V_2$ and $V_3$ constants. Recall that discontinuous solutions occur when $\theta(\sigma_1) = \theta(\sigma_2) = 0$, it implies

$$\theta_1(\sigma_1) = \theta_2(\sigma_1) = \theta_2(\sigma_2) = \theta_3(\sigma_2) = 0,$$

and thus, $\theta$ takes the following form

$$\frac{\theta^2}{2} = \begin{cases} \dfrac{\theta_1^2}{2} = k_1\Big[\phi(\xi) - \phi(\sigma_1) + \Big(k_1 - \dfrac{V_1^2}{2} - 2A_1 + E_1\Big)(\xi^2 - \sigma_1^2)\Big], & \xi \in (0, \sigma_1) \\ \dfrac{\theta_2^2}{2} = k_2\Big[\phi(\xi) - \phi(\sigma_1) - \dfrac{\phi(\sigma_2) - \phi(\sigma_1)}{\sigma_2^2 - \sigma_1^2}(\xi^2 - \sigma_1^2)\Big], & \xi \in (\sigma_1, \sigma_2) \\ \dfrac{\theta_3^2}{2} = k_3\Big[\phi(\xi) - \phi(\sigma_2) + \Big(k_3 - \dfrac{V_3^2}{2} - 2A_3 + E_3\Big)(\xi^2 - \sigma_2^2)\Big], & \xi \in (\sigma_2, \infty) \end{cases} \tag{4.16}$$

Imposing now the boundary conditions (3.6) into (4.16) yields the explicit formula of discontinuous solution $\theta$

$$\frac{\theta^2}{2} = \begin{cases} k_1\Big[\phi(\xi) - \phi(\sigma_1) - \dfrac{\xi^2 - \sigma_1^2}{\sigma_1^2}\phi(\sigma_1)\Big], & \xi \in (0, \sigma_1) \\ k_2\Big[\phi(\xi) - \phi(\sigma_1) - \dfrac{\phi(\sigma_2) - \phi(\sigma_1)}{\sigma_2^2 - \sigma_1^2}(\xi^2 - \sigma_1^2)\Big], & \xi \in (\sigma_1, \sigma_2) \\ k_3\Big[\phi(\xi) - \phi(\sigma_2)\Big], & \xi \in (\sigma_2, \infty) \end{cases} \tag{4.17}$$

Note that functions $\theta_1$ and $\theta_3$ have the same form as $\theta_-$ and $\theta_+$ in (4.11) for $\sigma = \sigma_1$ and $\sigma = \sigma_2$, respectively. Likewise $k_-$ and $k_+$, we conclude that $k_1 > 0$ and $k_3 > 0$ using the same reasoning. To define the sign of $k_2$ in the remaining case, we consider the following lemma.

**Lemma 4.3** *Let $\xi \in (\sigma_1, \sigma_2)$. Then,*

$$J(\xi) = \phi(\xi) - \phi(\sigma_1) - \frac{\phi(\sigma_2) - \phi(\sigma_1)}{\sigma_2^2 - \sigma_1^2}(\xi^2 - \sigma_1^2) > 0. \tag{4.18}$$

***Proof*** For $\xi \in (\sigma_1, \sigma_2)$, set

$$J(\xi) = \phi(\xi) - \phi(\sigma_1) - \frac{\phi(\sigma_2) - \phi(\sigma_1)}{\sigma_2^2 - \sigma_1^2}(\xi^2 - \sigma_1^2) = (\xi^2 - \sigma_1^2)\Big[F(\xi) - F(\sigma_2)\Big],$$

where $F(\xi) = \frac{\phi(\xi) - \phi(\sigma_1)}{\xi^2 - \sigma_1^2}$. From the mean value theorem, observe

$$F'(\xi) = \frac{1}{\xi^2 - \sigma_1^2}\left[\phi'(\xi) - \frac{2\xi}{\xi + \sigma_1}\frac{\phi(\xi) - \phi(\sigma_1)}{\xi - \sigma_1}\right] = \frac{1}{\xi^2 - \sigma_1^2}\left[\phi'(\xi) - \frac{2\xi}{\xi + \sigma_1}\phi'(c)\right],$$

where $c \in (\sigma_1, \xi)$. Recall Lemma (3.1), the concavity of $\phi$ implies that $F$ is decreasing

$$F'(\xi) \leq \frac{\phi'(c)}{\xi^2 - \sigma_1^2}\left[1 - \frac{2\xi}{\xi + \sigma_1}\right] < 0.$$

Hence, we get

$$\Big[F(\xi) - F(\sigma_2)\Big] > 0, \quad \xi \in (\sigma_1, \sigma_2),$$

which completes the proof. □

Lemma (4.3) implies that $k_2 > 0$. Considering the signs of constants $k_1$, $k_2$ and $k_3$, we proceed to the main theorem about the nonexistence of solutions with discontinuities at two points.

**Theorem 4.4** *Let $(\theta, V, P)$ be a weak solution of (3.1a)–(3.1c) of class $\theta \in W^{1,1}((0,\infty))$, $V \in BV((0,\infty)) \cap L^\infty((0,\infty))$ and $P \in BV((0,\infty)) \cap L^\infty((0,\infty))$ which satisfies the boundary conditions*

$$V(0+) = V_0, \quad P(0+) = E_0, \quad \theta(0) = 0, \quad \theta'(\infty) = 0.$$

*There does not exist a solution $(\theta, V, P)$ with discontinuities at two points that satisfies jump conditions (4.7).*

***Proof*** Suppose there exists a weak solution $\theta$ given by (4.17) that satisfies jump conditions (4.7) on both discontinuity points $\sigma_1$ and $\sigma_2$. Consider first the condition (4.7c) applied to (4.17) at $\xi = \sigma_1$. That is,

$$\theta_1(\sigma_1)\theta_1'(\sigma_1) = \theta_2(\sigma_1)\theta_2'(\sigma_1).$$

This yields a constrain on constants $k_1, k_2$

$$\frac{k_1}{k_2} = -\sqrt{1+\sigma_1^2}\left(1 - 2\frac{\phi(\sigma_2)-\phi(\sigma_1)}{\sigma_2^2-\sigma_1^2}\frac{\sigma_1}{\phi'(\sigma_1)}\right)\phi'(\sigma_1). \tag{4.19}$$

Note that $\phi'(\sigma_1) - 2\frac{\phi(\sigma_1)}{\sigma_1} = -\frac{1}{\sqrt{1+\sigma_1^2}}$.

Since $k_1 > 0$ and $k_2 > 0$, the relation (4.19) holds if and only if

$$1 - 2\frac{\phi(\sigma_2)-\phi(\sigma_1)}{\sigma_2^2-\sigma_1^2}\frac{\sigma_1}{\phi'(\sigma_1)} < 0. \tag{4.20}$$

Using the mean value theorem, one may rewrite (4.20) as

$$\begin{aligned} 0 > 1 - 2\frac{\phi(\sigma_2)-\phi(\sigma_1)}{\sigma_2^2-\sigma_1^2}\frac{\sigma_1}{\phi'(\sigma_1)} &= 1 - \frac{2\sigma_1}{\sigma_2+\sigma_1}\frac{\phi(\sigma_2)-\phi(\sigma_1)}{\sigma_2-\sigma_1}\frac{1}{\phi'(\sigma_1)} \\ &= 1 - \frac{2\sigma_1}{\sigma_2+\sigma_1}\frac{\phi'(c)}{\phi'(\sigma_1)} \end{aligned} \tag{4.21}$$

for $c \in (\sigma_1, \sigma_2)$. Recall $\phi(\xi)$ is concave, it implies that $\phi'(\sigma_1) > \phi'(c)$ and

$$1 - \frac{2\sigma_1}{\sigma_2+\sigma_1}\frac{\phi'(c)}{\phi'(\sigma_1)} > \frac{\sigma_2-\sigma_1}{\sigma_2+\sigma_1} > 0,$$

which contradicts (4.21). Hence, the jump condition (4.7c) is not satisfied at $\xi = \sigma_1$.

Next, we consider the condition (4.7c) applied to (4.17) at $\xi = \sigma_2$. That is,

$$\theta_3(\sigma_2)\theta_3'(\sigma_2) = \theta_2(\sigma_2)\theta_2'(\sigma_2).$$

This provides a restriction on constants $k_2, k_3$

$$\frac{k_3}{k_2} = 1 - 2\frac{\phi(\sigma_2)-\phi(\sigma_1)}{\sigma_2^2-\sigma_1^2}\frac{\sigma_2}{\phi'(\sigma_2)}. \tag{4.22}$$

Since $k_2 > 0$ and $k_3 > 0$, the relation (4.22) holds if and only if

$$1 - 2\frac{\phi(\sigma_2)-\phi(\sigma_1)}{\sigma_2^2-\sigma_1^2}\frac{\sigma_2}{\phi'(\sigma_2)} > 0.$$

From the mean value theorem, we obtain

$$0 < 1 - 2\frac{\phi(\sigma_2)-\phi(\sigma_1)}{\sigma_2^2-\sigma_1^2}\frac{\sigma_2}{\phi'(\sigma_2)} = 1 - \frac{2\sigma_2}{\sigma_2+\sigma_1}\frac{\phi'(c)}{\phi'(\sigma_2)},$$

for some $c \in (\sigma_1, \sigma_2)$. The concavity of $\phi$ leads again to a contradiction. Therefore, there does not exist a discontinuous solution $(\theta, V, P)$ with discontinuities at two points that satisfies the jump conditions (4.7). □

Recall Theorems 4.2 and 4.4, we observe that jump condition (4.7c) is not satisfied neither near the boundary nor across the vortex line, despite the existence of an intermediate region. Therefore, a similar outcome will also be obtained if a finite number of intermediate layers are considered. This leads to the following corollary.

**Corollary 4.5** *Let* $(\theta, V, P)$ *be a weak solution of* (3.1a)–(3.1c) *of class* $\theta \in W^{1,1}((0,\infty))$, $V \in BV((0,\infty)) \cap L^{\infty}((0,\infty))$ *and* $P \in BV((0,\infty)) \cap L^{\infty}((0,\infty))$ *which satisfies the boundary conditions*

$$V(0+) = V_0, \quad P(0+) = E_0, \quad \theta(0) = 0, \quad \theta'(\infty) = 0.$$

*There does not exist a solution* $(\theta, V, P)$ *with discontinuities at a finite number of points that fulfils the jump conditions* (4.7).

### 4.2 Interaction of Vortex with Boundary

Motivated by the study of Euler equations presented in the previous sections, we are interested in extending it to a class of flows where there is mass input or loss through the vortex line. In other words, we assume that the vortex line can be either a source or a sink of the fluid motion. Since that the vortex line resembles the tornado core, this assumption is not unnatural for a tornado-like flow. In terms of the self-similar functions (2.10), the assumption leads to

$$U(\xi) \to U_{\infty} \quad \text{as} \quad \xi \to \infty,$$

or in terms of $\theta$

$$\theta'(\xi) \to -U_{\infty} \quad \text{as} \quad \xi \to \infty, \tag{4.23}$$

where $U_{\infty}$ is a nonzero constant.

#### 4.2.1 Continuous Solutions

Consider first the case where solutions are continuous. Same calculations as those described in Sect. 3 lead again to solutions in form (3.4). The boundary condition (4.23) on the vortex line applied to (3.4a) yields

$$\frac{1}{2}U_{\infty}^2 = k_0 - \frac{V_0^2}{2} - 2A_0 + E_0. \tag{4.24}$$

To derive this, note that (3.4a) implies

$$\theta' = \frac{1}{\theta}\left[k_0\phi'(\xi) + 2\left(k_0 - \frac{V_0^2}{2} - 2A_0 + E_0\right)\xi\right] \xrightarrow{\xi\to\infty} \pm\sqrt{2\left(k_0 - \frac{V_0^2}{2} - 2A_0 + E_0\right)}.$$

Thus, as $\xi \to \infty$

$$\theta'(\infty) = -U_\infty = \pm\sqrt{2\left(k_0 - \frac{V_0^2}{2} - 2A_0 + E_0\right)}.$$

In addition, we impose a no-penetration boundary condition at $\xi = 0$, i.e. $\theta(0) = 0$. Applying this to (3.4a) provides

$$A_0 = E_0. \tag{4.25}$$

As a result the relation (4.24) reduces to

$$\frac{1}{2}U_\infty^2 = k_0 - \frac{V_0^2}{2} - E_0. \tag{4.26}$$

Substituting (4.25) and (4.26) into (3.4), we obtain an explicit family solutions of (3.1a-(3.1c)) depending on parameters $U_\infty$, $V_0$ and $E_0$

$$\frac{\theta^2}{2} = k_0\phi(\xi) + \frac{1}{2}U_\infty^2\xi^2, \qquad U = -\frac{1}{\theta}\left[\frac{k_0}{\sqrt{1+\xi^2}}\left(1 - 2\phi(\xi)\right) + U_\infty^2\xi\right], \tag{4.27a}$$

$$V = V_0, \qquad W = \frac{k_0}{\theta}\frac{\xi}{\sqrt{1+\xi^2}}, \qquad P = E_0 - k_0\frac{\xi}{\sqrt{1+\xi^2}}, \tag{4.27b}$$

where

$$k_0 = \frac{1}{2}U_\infty^2 + \frac{V_0^2}{2} + E_0.$$

We next investigate the existence of discontinuous solutions in this framework.

#### 4.2.2 Nonexistence of Discontinuous Solutions

Let $(\theta, V, P)$ be a weak solution of (3.1a)–(3.1d) with a discontinuity at a fixed point $\xi = \sigma$, $\sigma \in (0, \infty)$, which satisfies the boundary condition (4.23). This suggests seeking solutions in the form

$$\theta(\xi) = \begin{cases} \theta_-(\xi), \\ \theta_+(\xi) \end{cases} \quad \text{and} \quad V(\xi) = \begin{cases} V_-(\xi), & \xi \in (0, \sigma) \\ V_+(\xi), & \xi \in (\sigma, \infty) \end{cases}$$

Repeating calculations described in Sect. 3, we obtain again solutions in form (3.4a) on $(0, \sigma)$ and $(\sigma, \infty)$, respectively. The system (3.1a)–(3.1c) is solved on each domain independently. Note that $V(\xi)$ is again a constant function with $V_-$ and $V_+$ constants. Recall that discontinuous solutions occur when $\theta(\sigma) = 0$, the relation for $\theta$ becomes

$$\frac{\theta_\pm^2}{2} = k_\pm\Big(\phi(\xi) - \phi(\sigma)\Big) + \Big(k_\pm - \frac{V_\pm^2}{2} - 2A_\pm + E_\pm\Big)\big(\xi^2 - \sigma^2\big). \tag{4.28}$$

where $k_\pm$, $A_\pm$ and $E_\pm$ are integration constants.

We impose a no-penetration boundary condition at the boundary and the condition (4.23) at the vortex line, namely

$$\theta_-(0) = 0, \quad \text{and} \quad \theta'_+(\xi) \to -U_\infty \quad \text{as} \quad \xi \to \infty,$$

which imply

$$k_- - \frac{V_-^2}{2} - 2A_- + E_- = -k_- \frac{1}{\sigma^2}, \tag{4.29}$$

$$k_+ - \frac{V_+^2}{2} - 2A_+ + E_+ = \frac{1}{2}U_\infty^2. \tag{4.30}$$

To derive (4.30), note that (4.28) provides

$$\theta'_+ \xrightarrow{\xi\to\infty} \pm\sqrt{2\left(k_+ - \frac{V_+^2}{2} - 2A_+ + E_+\right)},$$

and thus,

$$\theta'_+(\infty) = -U_\infty = \pm\sqrt{2\left(k_+ - \frac{V_+^2}{2} - 2A_+ + E_+\right)}.$$

Substituting (4.29) and (4.30) into (4.28), we obtain the explicit formula

$$\frac{\theta^2}{2} = \begin{cases} k_-\left[\phi(\xi) - \phi(\sigma) - \dfrac{\xi^2 - \sigma^2}{\sigma^2}\phi(\sigma)\right], & \xi \in (0, \sigma) \\ k_+\left[\phi(\xi) - \phi(\sigma)\right] + \dfrac{1}{2}U_\infty^2(\xi^2 - \sigma^2), & \xi \in (\sigma, \infty) \end{cases} \tag{4.31}$$

where $k_+$, $k_-$ are constants. From (3.4) and (4.31), one may derive the explicit formulas of discontinuous solutions $U$, $W$ and $P$.

Examining now whether discontinuous solutions in the form (4.31) are feasible leads to the following theorem.

**Theorem 4.6** *Let $(\theta, V, P)$ be a weak solution of (3.1a)–(3.1c) of class $\theta \in W^{1,1}((0,\infty))$, $V \in BV((0,\infty)) \cap L^\infty((0,\infty))$ and $P \in BV((0,\infty)) \cap L^\infty((0,\infty))$ which satisfies the boundary conditions*

$$V(0+) = V_0, \quad P(0+) = E_0, \quad \theta(0) = 0, \quad \theta'(\infty) = U_\infty.$$

*There does not exist a solution $(\theta, V, P)$ with a discontinuity at a single point that fulfils jump conditions (4.7).*

***Proof*** Suppose $\theta$ is a weak solution given by (4.31) that satisfies jump conditions (4.7). Then (4.7c) applied to (4.31) provides a constraint between the constants $k_+, k_-$ and the parameter $U_\infty^2$,

$$-k_+\phi'(\sigma) = k_-\Big(2\frac{\phi(\sigma)}{\sigma} - \phi'(\sigma)\Big) + U_\infty^2\sigma. \tag{4.32}$$

Using (3.9) we compute $2\frac{\phi(\sigma)}{\sigma} - \phi'(\sigma) = \frac{1}{\sqrt{1+\sigma^2}} > 0$.

Since $\theta^2(\xi) > 0$ for $\xi \neq \sigma$, relation (4.31) imposes restrictions on the signs of $k_+, k_-$. First, observe that $\frac{\theta^2}{2}(\xi) = k_- J(\xi)$ where $J(\xi)$ is given by (4.14). Since $J(\xi) > 0$ for $\xi \in (0, \sigma)$, it implies that $k_- > 0$.

If it were $k_+ > 0$ this would contradict (4.32). Consider now the possibility that the constants are $k_- > 0$, $k_+ < 0$. Then (4.31) dictates that

$$k_+\frac{\phi(\xi) - \phi(\sigma)}{\xi - \sigma} + \frac{1}{2}U_\infty^2(\xi + \sigma) > 0 \quad \text{for } \xi > \sigma.$$

The latter implies, as $\xi \to \sigma_+$,

$$k_+\phi'(\sigma) + U_\infty^2\sigma \geq 0$$

and contradicts via (4.32) that $k_- > 0$. Hence, there does not exist a discontinuous solution $(\theta, V, P)$ that fulfils the jump conditions (4.7). □

## 5 Stationary Self-Similar Axisymmetric Navier–Stokes Equations

In this section we study self-similar solutions for the stationary axisymmetric Navier–Stokes equations (1.1). The *ansatz* (2.10) leads to the system (2.14) in the variables $(\theta, V, P)$, where the velocities $(U, W)$ are determined from the stream function $\theta$ via (2.13). We first provide a convenient reformulation of (2.14) as a coupled integrodifferential system and then study the limiting behaviour as the viscosity $\nu \to 0$, the form of the boundary layer, and identify conditions on admissible solutions of the Euler equations.

### 5.1 Formulation via an Integrodifferential System

The system (2.14) for $\nu > 0$ gives after an integration

$$\frac{\theta^2}{2} + (1+\xi^2)P = \nu\Big[\xi\theta - (1+\xi^2)\theta'\Big] - \int_0^\xi sV^2\,\mathrm{d}s + A_0\,, \tag{5.1a}$$

$$\theta^2 - \xi\Big(\frac{\theta^2}{2}\Big)' + P = \nu\Big[\xi\theta - \xi^2\theta' - \xi(1+\xi^2)\theta''\Big] + E_0, \tag{5.1b}$$

where $A_0$, $E_0$ are integration constants.

We impose a no-slip boundary condition $\vec{u} = 0$ at the boundary $z = 0$, which implies $u = v = w = 0$ at $z = 0$. Expressed in terms of self-similar functions it yields

$$U(0) = V(0) = W(0) = 0, \quad \text{and thus} \quad \theta(0) = \theta'(0) = 0. \tag{5.2}$$

We also require that no mass is added or lost through the vortex line, that is at the height $z$ the mass flux per unit height $\int_0^{2\pi} u(r, \theta, z)\, r \mathrm{d}\theta \to 0$ as $r \to 0$. In the self-similar, stationary setting (2.10) the condition at the vortex core becomes

$$U = -\theta' \to 0 \quad \text{as } \xi \to \infty. \tag{5.3}$$

Since (2.14b) is second order, an additional condition is required for $V(\xi)$. We request the vortex line to have constant swirl:

$$V \to V_\infty, \text{ as } \xi \to \infty. \tag{5.4}$$

Then (5.2) together with (5.1a) and (5.1b) imply that $E_0 = A_0 = P(0)$. Eliminating $P$ from (5.1a) and (5.1b) gives

$$\begin{aligned} &\xi(1+\xi^2)\Big(\frac{\theta^2}{2}\Big)' - (1+2\xi^2)\frac{\theta^2}{2} + \nu\Big[\xi^3\theta + (1-\xi^4)\theta' - \xi(1+\xi^2)^2\theta''\Big] \\ &\quad = -\int_0^\xi s V^2 \,\mathrm{d}s - E_0\xi^2. \end{aligned}$$

Upon dividing by $\xi^2(1+\xi^2)^{\frac{3}{2}}$ and using the calculus identities

$$\frac{\mathrm{d}}{\mathrm{d}\xi}\frac{1}{\xi(1+\xi^2)^{\frac{1}{2}}} = -\frac{1+2\xi^2}{\xi^2(1+\xi^2)^{\frac{3}{2}}} \qquad \frac{\mathrm{d}}{\mathrm{d}\xi}\frac{(1+\xi^2)^{\frac{1}{2}}}{\xi} = -\frac{1}{\xi^2(1+\xi^2)^{\frac{1}{2}}} \tag{5.5}$$

$$\frac{\mathrm{d}}{\mathrm{d}\xi}\frac{1}{(1+\xi^2)^{\frac{1}{2}}} = -\frac{\xi}{(1+\xi^2)^{\frac{3}{2}}} \qquad \frac{\mathrm{d}}{\mathrm{d}\xi}\Big(\frac{1}{\xi\sqrt{1+\xi^2}\big(\xi+\sqrt{1+\xi^2}\big)^2}\Big) = -\frac{1}{\xi^2(1+\xi^2)^{\frac{3}{2}}} \tag{5.6}$$

we obtain after some rearrangements the equation

$$\begin{aligned} \frac{\mathrm{d}}{\mathrm{d}\xi}\left(\frac{1}{\xi\sqrt{1+\xi^2}}\frac{\theta^2}{2} - \nu\Big[\frac{1}{\sqrt{1+\xi^2}}\theta + \frac{\sqrt{1+\xi^2}}{\xi}\theta'\Big]\right) &= -\frac{1}{\xi^2(1+\xi^2)^{\frac{3}{2}}}\int_0^\xi s V^2 \,\mathrm{d}s \\ &\quad - \frac{\mathrm{d}}{\mathrm{d}\xi}\Big(\frac{E_0\xi}{(1+\xi^2)^{\frac{1}{2}}}\Big). \end{aligned} \tag{5.7}$$

Using the boundary condition (5.3), $\theta'(\infty) = 0$, which also implies that $\lim_{\xi\to\infty} \frac{\theta(\xi)}{\xi} = 0$, we integrate (5.7) over the interval $(\xi, \infty)$ to obtain

$$\frac{\theta^2}{2} - \nu\Big(1+\xi^2)\theta' + \xi\theta\Big) = \xi(1+\xi^2)^{\frac{1}{2}} \int_\xi^\infty \frac{1}{\zeta^2(1+\zeta^2)^{\frac{3}{2}}} \Big( \int_0^\zeta sV^2(s)\mathrm{d}s \Big)\mathrm{d}\zeta + E_0\Big(\xi(1+\xi^2)^{\frac{1}{2}} - \xi^2\Big).$$

The latter is an integrodifferential equation depending on $\mathcal{G}(V;\xi)$ a functional on $V$,

$$\begin{aligned} \mathcal{G}(V;\xi) &:= \xi\sqrt{1+\xi^2} \int_\xi^\infty \frac{1}{\zeta^2(1+\zeta^2)^{\frac{3}{2}}} \Big( \int_0^\zeta sV^2(s)\mathrm{d}s \Big)\mathrm{d}\zeta \\ &= \xi\sqrt{1+\xi^2} \int_\xi^\infty \frac{1}{s\sqrt{1+s^2}\big(s+\sqrt{1+s^2}\big)^2} sV^2\mathrm{d}s \\ &\quad + \frac{1}{(\xi+\sqrt{1+\xi^2})^2} \int_0^\xi sV^2\mathrm{d}s, \end{aligned} \tag{5.8}$$

where the last equality follows via integration by parts using (5.6).

In summary, the system (2.14) with boundary conditions (5.2)–(5.4) is transformed to a coupled integrodifferential system for $(\theta, V)$,

$$\frac{\theta^2}{2} - \nu\Big[(1+\xi^2)\theta' + \xi\theta\Big] = \mathcal{G}(V;\xi) + E_0\phi(\xi) \tag{5.9a}$$

$$\nu(1+\xi^2)V'' + \Big(3\nu\xi - \theta\Big)V' = 0\,, \tag{5.9b}$$

where $\mathcal{G}(V;\xi)$ is the functional in (5.8) and $\phi(\xi)$ the function in (3.9) that played a prominent role in the Euler equations. The system is supplemented with the boundary conditions

$$\theta(0) = V(0) = 0, \quad \text{at} \quad \xi = 0\,, \tag{5.10a}$$

$$V \to V_\infty, \quad \text{as} \quad \xi \to \infty. \tag{5.10b}$$

and satisfies $\theta'(0) = \theta'(\infty) = 0$. The parameter $E_0 = P(0)$ reflects on the pressure $p = \frac{1}{r^2}P(\xi)$ and $P$ may be computed by (5.1b).

### 5.2 Alternative Equivalent Formulations

Next, we derive two more equivalent formulations of the system (5.9) with simpler structure. This will benefit the analysis and provides a different perspective on the problem.

First we set

$$\hat\theta(\xi) = \sqrt{1+\xi^2}\,\theta(\xi) \quad \text{and} \quad \hat V(\xi) = V(\xi), \quad \xi \in [0,\infty), \tag{5.11}$$

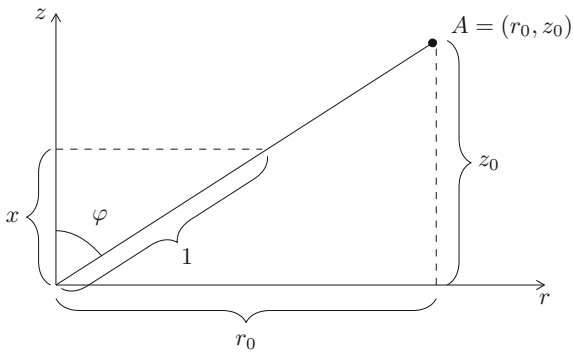


**Fig. 5** Coordinate System

and obtain

$$\frac{\hat{\theta}^2}{2} - \nu(1+\xi^2)^{\frac{3}{2}}\,\hat{\theta}' = (1+\xi^2)\Big(\mathcal{G}\big(\hat{V}(\xi);\xi\big) + E_0\phi(\xi)\Big), \tag{5.12a}$$

$$\nu\Big((1+\xi^2)^{\frac{3}{2}}\,\hat{V}'\Big)' = \hat{\theta}\,\hat{V}', \tag{5.12b}$$

with boundary conditions (5.10).

An alternative form of (5.9) is derived by introducing a change of variable $\xi \to x$ such that $\frac{\mathrm{d}}{\mathrm{d}x} = (1+\xi^2)^{\frac{3}{2}}\frac{\mathrm{d}}{\mathrm{d}\xi}$. This is achieved by defining $x$ by

$$x = \frac{\xi}{\sqrt{1+\xi^2}} \quad \text{with inverse transformation} \quad \xi = \frac{x}{\sqrt{1-x^2}}. \tag{5.13}$$

The change of variables $\xi \to x$ is a surjective map $T : [0,\infty) \to [0,1)$ and has an interpretation as a change from cylindrical $(r,\vartheta,z)$ to spherical $(\rho,\vartheta,\varphi)$ coordinates, see Fig. 5. Since $\xi = \frac{z}{r}$, it follows $\xi = \frac{\cos\varphi}{\sin\varphi} = \cot\varphi$ and setting $x = \cos\varphi$ yields

$$\xi = \frac{\cos\varphi}{\sin\varphi} = \frac{x}{\sqrt{1-x^2}}. \tag{5.14}$$

The functions $\hat{\theta}(\xi)$ and $\hat{V}(\xi)$ are expressed in terms of the variable $x$ as follows

$$\Theta(x) = \hat{\theta}(\xi) \quad \text{and} \quad V(x) = \hat{V}(\xi), \tag{5.15}$$

where $\xi$, $x$ are related via (5.13).

Using the transformation (5.13), (5.15), the system (5.9) reduces to the equivalent form

$$\nu\,\frac{\mathrm{d}\Theta}{\mathrm{d}x} = \frac{\Theta^2(x)}{2} - \mathcal{F}\,(V;x)\,, \tag{5.16a}$$

$$\nu\frac{\mathrm{d}^2V}{\mathrm{d}^2x} = \Theta(x)\,\frac{\mathrm{d}V}{\mathrm{d}x}, \tag{5.16b}$$

$$\Theta(0) = V(0) = 0, \tag{5.16c}$$

$$V \to V_\infty, \quad \text{as } x \to 1, \tag{5.16d}$$

where $\mathcal{F}$ is

$$\begin{aligned}
\mathcal{F}(V;x) &:= (1+\xi^2)\Big(\mathcal{G}\big(\hat{V}(\xi);\xi\big) + E_0\phi(\xi)\Big)\Big|_{\xi=\frac{x}{\sqrt{1-x^2}}} \\
&= \frac{x}{(1-x^2)^2}\int_x^1 \frac{1-t^2}{t^2}\left(\int_0^{\frac{t}{\sqrt{1-t^2}}} s\hat{V}^2(s)\mathrm{d}s\right)\mathrm{d}t + E_0\,\frac{x-x^2}{(1-x^2)^2} \\
&= \frac{x}{(1-x^2)^2}\left[\int_x^1 \frac{1-t^2}{t^2}\left(\int_0^t \frac{\sigma}{(1-\sigma^2)^2}V^2(\sigma)\mathrm{d}\sigma\right)\mathrm{d}t + E_0\,(1-x)\right] \\
&= \frac{1}{(1-x^2)^2}\left[x\int_x^1 \frac{1}{(t+1)^2}V^2(t)\mathrm{d}t\right. \\
&\quad \left. + (1-x)^2\int_0^x \frac{t}{(1-t^2)^2}V^2(t)\mathrm{d}t + E_0\,x(1-x)\right]
\end{aligned} \tag{5.17}$$

The first expression in (5.17) is the definition of $\mathcal{F}(V;x)$, and the remaining equalities are obtained using (3.9), (5.8), the change of variables $\xi = \frac{x}{\sqrt{1-x^2}}$ and the formula $V(x) = \hat{V}\left(\frac{x}{\sqrt{1-x^2}}\right)$ connecting $V(x)$ defined on $[0,1)$ with $\hat{V}(\xi)$ defined on $[0,\infty)$.

Variants of (5.16) appear in Goldshtik (1960), Serrin (1972), Shtern and Hussain (1999), Fernandez-Feria and Arrese (2000), Bělík et al. (2014) originating from different authors who initiate their studies by considering either spherical or cylindrical coordinates. Serrin (1972) provided a detailed analysis of existence of solutions for (5.16) and a (indicative) bifurcation diagram for solutions. We refer to Sect. 7 for numerical computations leading to a computational bifurcation diagram, see Fig. 11. As $\Theta$ satisfies a Riccati-type equation, there are regions of $\nu$ for which $\Theta(x)$ blows up for $x \in [0,1)$ leading to nonexistence of solutions for such $\nu$. This is explained in the following section.

### 5.3 Properties and A Priori Estimates

In the sequel we are interested in the limit $\nu \to 0$ and the convergence of (5.16) to solutions of the Euler equations. To fix ideas we restrict to the case $V_\infty > 0$. Then (5.16b), (5.16d) imply that $V(x)$ is strictly increasing and yields the representation formula

$$V(x) = V_\infty \frac{\int_0^x e^{\frac{1}{\nu}\int_0^t \Theta(s)\mathrm{d}s}\mathrm{d}t}{\int_0^1 e^{\frac{1}{\nu}\int_0^t \Theta(s)\mathrm{d}s}\mathrm{d}t} \tag{5.18}$$

leading to the following lemma.

**Lemma 5.1** *When $V_\infty > 0$ the function $V(x)$ is strictly increasing and satisfies $0 < V(x) < V_\infty$ independently of $\nu > 0$.*

We turn next to the equation (5.16a),

$$\nu \frac{\mathrm{d}\Theta}{\mathrm{d}x} = \frac{\Theta^2(x)}{2} - \frac{x}{(1-x^2)^2}\Big(H(x) + E_0\,(1-x)\Big) \tag{5.19}$$

and proceed to establish properties for $\Theta$. The functional $H(x)$ in (5.17) is given by

$$H(x) = \int_x^1 \frac{1-t^2}{t^2}\left(\int_0^{\frac{t}{\sqrt{1-t^2}}} s\hat{V}^2(s)\mathrm{d}s\right)\mathrm{d}t, \tag{5.20}$$

here expressed in terms of the velocity $\hat{V}(\xi)$ defined on $(0,\infty)$. The derivatives of $H(x)$ are

$$\frac{\mathrm{d}H}{\mathrm{d}x}(x) = -\frac{1-x^2}{x^2}\int_0^{\frac{x}{\sqrt{1-x^2}}} s\hat{V}^2(s)\mathrm{d}s < 0, \quad x \in [0,1), \tag{5.21}$$

$$\frac{\mathrm{d}^2H}{\mathrm{d}x^2}(x) = -\frac{2}{x^3}\int_0^{\frac{x}{\sqrt{1-x^2}}} s\hat{V}(s)\frac{\mathrm{d}\hat{V}}{\mathrm{d}s}(s)\mathrm{d}s < 0, \quad x \in [0,1), \tag{5.22}$$

and $H(x)$ satisfies

$$0 < H(0) = \int_0^1 \frac{1-t^2}{t^2}\left(\int_0^{\frac{t}{\sqrt{1-t^2}}} s\hat{V}^2(s)\mathrm{d}s\right)\mathrm{d}t < \frac{V_\infty^2}{2}, \tag{5.23}$$

$H(1) = 0$, $\lim_{x\to 0}\frac{\mathrm{d}H}{\mathrm{d}x} = 0$ and $\lim_{x\to 0}\frac{\mathrm{d}^2H}{\mathrm{d}x^2} = 0$. Hence, $H(x)$ is decreasing and concave. A sketch of $H(x)$ is presented in Fig. 6. If we define

$$\frac{\mathrm{d}H}{\mathrm{d}x}(1) = -\lim_{\xi\to\infty}\frac{1}{\xi^2}\int_0^\xi s\hat{V}^2(s)\mathrm{d}s =: -\beta < 0 \tag{5.24}$$

we observe that due to the concavity of $H(x)$ we have the bounds

$$H(0)(1-x) \le H(x) \le \beta(1-x) \qquad x \in [0,1] \tag{5.25}$$

with $H(0)$, $\beta$ defined in (5.23), (5.24) and satisfying $H(0) < \beta$.

As a consequence, the function $F = H + E_0(1-x)$ in the Riccati-type equation (5.19) obeys the bounds

$$(H(0)+E_0)(1-x) \le F(x) = H(x) + E_0(1-x) \le (\beta+E_0)(1-x) \tag{5.26}$$

and resembles one of the following configurations, see Fig. 7:

(a) $F$ in negative on $[0,1]$, which occurs when $\beta + E_0 < 0$.

**Fig. 6** $H(x)$

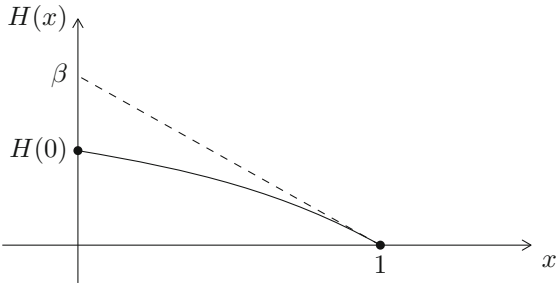


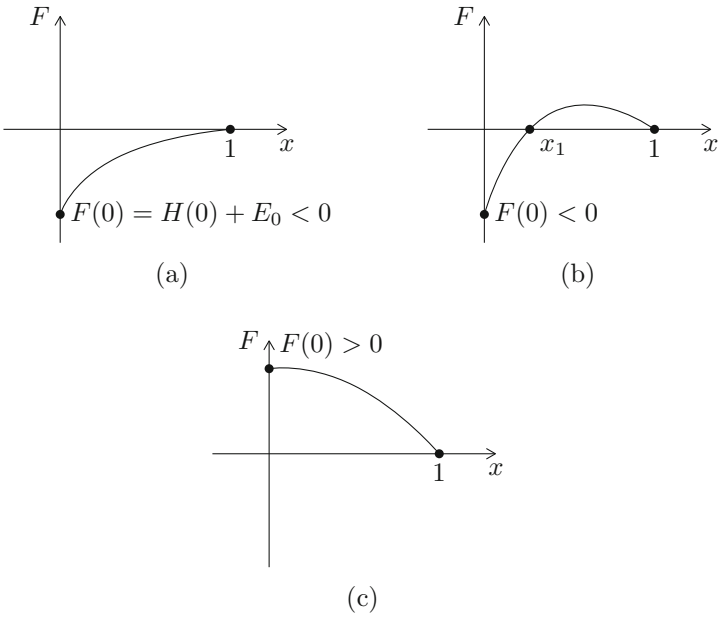


**Fig. 7** Possible configuration of function $F$

(b) $F$ is first negative, it becomes zero at a point $0 < x_1 < 1$ and then $F$ is positive. This occurs when $H(0) + E_0 < 0 < \beta + E_0$.
(c) $F$ in positive for $[0, 1)$, occurring when $0 < H(0) + E_0$.

This restricts considerably the possible shapes of $\Theta$. A computation using (5.19) gives

$$\nu \frac{\mathrm{d}^2\Theta}{\mathrm{d}x^2}(0) = -(H(0) + E_0) = -F(0).$$

Since $\Theta(0) = \frac{\mathrm{d}\Theta}{\mathrm{d}x}(0) = 0$ the value of $F(0)$ determines in which half-plane $\Theta(x)$ initially starts. Consider first the case where $F(0) = H(0) + E_0 > 0$. Then $F(x) > 0$ for all $x \in (0, 1)$, that is the setting of case $(c)$, illustrated in Fig. 7c. $\Theta(x)$ starts in the

lower half-plane. If it crosses the x-axis at some point $x_1 < 1$, then

$$0 \le \nu \frac{\mathrm{d}\Theta}{\mathrm{d}x}(x_1) = -\frac{x_1}{(1-x_1^2)^2} F(x_1)$$

contradicting $F(x) > 0$. Therefore, when $H(0) + E_0 > 0$, the function $\Theta(x)$ remains negative for all $x \in (0, 1)$.

Next, consider the case $H(0) + E_0 < 0$ which corresponds to the cases $(a)$ or $(b)$. We now have

$$\nu \frac{\mathrm{d}^2\Theta}{\mathrm{d}x^2}(0) = -\Big(H(0) + E_0\Big) > 0$$

and $\Theta(x)$ starts at the upper half-plane. If $\Theta$ crosses the x-axis at some point $x_1 < 1$ then

$$0 \ge \nu \frac{\mathrm{d}\Theta}{\mathrm{d}x}(x_1) = -\frac{x_1}{(1-x_1^2)^2} F(x_1). \tag{5.27}$$

It is possible to cross going downwards, but it is not possible to cross a second time going upwards again. We conclude that when case $(b)$ happens, then $\Theta(x)$ can possibly cross the axis, but it cannot cross a second time. By contrast when case $(a)$ happens, (5.27) contradicts $F(x) < 0, x \in (0, 1)$, i.e. $\Theta(x)$ cannot cross the axis. In this regime, the differential inequality

$$\nu \frac{\mathrm{d}^2\Theta}{\mathrm{d}x^2} > \frac{1}{2}\Theta^2, \quad x \in [0, 1)$$

implies that the solution $\Theta(x)$ blows up in finite time, and if $\nu$ is sufficiently small, this will happen within the interval $[0, 1]$.

Summarizing there are the following possibilities: When $F(x) > 0$ as in Fig. 7c then $\Theta(x) < 0$; when $F(x) < 0$ as in Fig. 7a then $\Theta(x) > 0$. When $F(x)$ changes sign as in Fig. 7b, then $\Theta$ starts at the upper half-plane, and either $\Theta$ stays there afterwards or it might cross to the lower half-plane. Accordingly, there are the following configurations: Either $\Theta(x) < 0$ which is called Zone A; or it starts with $\Theta(x) > 0$ but crosses to the negative half-plane and stays there thereafter, called Zone B, or it starts and stays $\Theta(x) > 0$, called Zone C. In Zone C, the solution $\Theta$ lies in the upper half-plane, and if $\nu$ is sufficiently small, it will blow up before reaching $x = 1$.

A-priori estimates for $\Theta(x)$ are derived below.

**Lemma 5.2** (i) *If $E_0 > 0$, then*

$$\Theta(x) < 0, \qquad 0 < x < 1$$

(ii) *If $\beta + E_0 > 0$, with $\beta$ defined in (5.24), then*

$$\Theta(x) > -\sqrt{2(\beta + E_0)}\ \frac{\sqrt{x - x^2}}{1 - x^2}, \qquad 0 < x < 1.$$

***Proof*** Note that $\Theta(0) = \frac{\mathrm{d}\Theta}{\mathrm{d}x}(0) = 0$ and $\frac{\mathrm{d}^2\Theta}{\mathrm{d}x^2}(0) = -\frac{H(0)+E_0}{\nu} < 0$ since $H(0)+E_0 > 0$. If the solution crosses to the upper half-plane, there exists $x_1 \in (0,1)$ such that $\Theta(x_1) = 0$, $\frac{\mathrm{d}\Theta}{\mathrm{d}x}(x_1) > 0$ and

$$\nu \frac{\mathrm{d}\Theta}{\mathrm{d}x}(x_1) = \frac{\Theta^2(x_1)}{2} - \frac{x_1}{(1-x_1^2)^2}\Big[H(x_1) + E_0\ (1-x_1)\Big]$$

This contradicts $H(x_1) > 0$ and $E_0 > 0$. Hence, $\Theta$ remains negative for all $x \in (0,1)$.

Let now $E_0 + \beta > 0$ and set $K = 2(E_0 + \beta)$, $\alpha(x) = \frac{\sqrt{x-x^2}}{1-x^2}$. Then (5.19) and (5.26) imply

$$\begin{aligned}
\nu \frac{\mathrm{d}\Theta}{\mathrm{d}x} &= \frac{\Theta^2(x)}{2} - \frac{x}{(1-x^2)^2}\Big[H(x) + E_0\ (1-x)\Big], \\
&\geq \frac{\Theta^2(x)}{2} - \frac{1}{2}K\frac{x(1-x)}{(1-x^2)^2} \\
&= \frac{1}{2}\Big(\Theta^2(x) - K\,\alpha^2(x)\Big)
\end{aligned} \tag{5.28}$$

Consider now the quantity $Z(x) := \Theta(x) + \sqrt{K}\ \alpha(x)$ and note that $\alpha(x) > 0$, $\dfrac{\mathrm{d}\alpha}{\mathrm{d}x} > 0$. Using (5.28), we obtain

$$\nu \frac{\mathrm{d}Z}{\mathrm{d}x} > \frac{1}{2}\big(\Theta - \sqrt{K}\,\alpha(x)\big)\,Z(x).$$

Since $Z(0) = \Theta(0) + \sqrt{K}\ \alpha(0) = 0$, we conclude that $Z(x) > 0$. □

When the bounds of Lemma 5.2 hold, the solution $\Theta$ of (5.19) cannot blow up in $(0,1)$. The hypothesis $\beta + E_0 > 0$, and thus, item (ii) of Lemma 5.2 is of theoretical interest, as the parameter $\beta$ cannot be a-priori determined. Nevertheless, using the bound $H(x) < \frac{1}{2}V_\infty^2$, we can prove a variant of (ii) providing a bound from below.

**Corollary 5.3** *If* $E_0 + \frac{1}{2}V_\infty^2 > 0$ *then*

$$\Theta(x) > -\sqrt{2E_0 + V_\infty^2}\ \frac{\sqrt{x-x^2}}{1-x^2}, \qquad 0 < x < 1.$$

*independently of* $\nu > 0$.

### 5.4 Convergence as $\nu \to 0$

Let $\left\{(\Theta_\nu, V_\nu)\right\}_{\nu>0}$ be a family of solutions of (5.16),

$$\begin{aligned} \nu \frac{\mathrm{d}\Theta_\nu}{\mathrm{d}x} &= \tfrac{1}{2}\Theta_\nu^2 - \mathcal{F}(V_\nu; x), \\ \nu \frac{\mathrm{d}^2 V_\nu}{\mathrm{d}^2 x} &= \Theta_\nu \frac{\mathrm{d}V_\nu}{\mathrm{d}x}, \end{aligned} \tag{5.29}$$

with $\nu > 0$ and we are interested in the limit $\nu \to 0$. Recall that, by $(5.17)_3$,

$$\mathcal{F}(V; x) = \frac{x}{(1-x^2)^2}\Big(H(V; x) + E_0(1-x)\Big) \tag{5.30}$$

$$\text{where} \quad H(V; x) = \int_x^1 \frac{1-t^2}{t^2} \int_0^t \frac{\sigma}{(1-\sigma^2)^2} V^2(\sigma)\mathrm{d}\sigma. \tag{5.31}$$

We assume that $\kappa := 2E_0 + V_\infty^2 > 0$ and that the family $(\Theta_\nu, V_\nu)$ satisfies the uniform bound

$$-\sqrt{\kappa}\,\frac{\sqrt{x(1-x)}}{1-x^2} < \Theta_\nu(x) < 0, \quad \text{for } x \in (0,1). \tag{B}$$

The assumption $\kappa > 0$ is natural since only then solutions of stationary self-similar axisymmetric Euler equations exist, see Sects. 3 and 4.

Regarding the uniform bounds (B): The left-hand inequality is guaranteed by Corollary 5.3, while the right-hand inequality follows from Lemma 5.2 in the more restrictive range $E_0 > 0$. The reader should note, that, as expected from numerical computations in the parameter range $\kappa > 0$, the solution of (5.29) enters Zone A—the region that $\Theta(x) < 0$—as $\nu$ decreases and stays there. This is corroborated by the bifurcation diagram sketched in Fig. 11.

Without loss of generality, we will examine the case $V_\infty > 0$. Then (5.16b) implies

$$\frac{\mathrm{d}V_\nu}{\mathrm{d}x} = V_\infty \frac{e^{\frac{1}{\nu}\int_0^x \Theta_\nu(s)\mathrm{d}s}}{\int_0^1 e^{\frac{1}{\nu}\int_0^t \Theta_\nu(s)\mathrm{d}s}\mathrm{d}t} > 0 \tag{5.32}$$

$$0 < V_\nu(x) < V_\infty, \quad x \in (0,1). \tag{5.33}$$

The sequence $\{V_\nu\}$ is of bounded variation, and by Helly's theorem it admits a convergent subsequence (which will be still denoted by $V_\nu$) such that

$$V_\nu(x) \to V(x) \quad a.e \ \ x \in (0,1). \tag{5.34}$$

For the sequence $\{\Theta_\nu\}$ the uniform bound implies that for $p \in [1,2)$

$$\int_0^1 |\Theta_\nu(x)|^p dx \le C \int_0^1 (1-x)^{-\frac{p}{2}}\mathrm{d}x =: K < \infty.$$

Using weak convergence techniques (Brezis 2010), there exist a subsequence (still denoted by $\Theta_\nu$) and a function $\Theta \in L^p(0,1)$ such that

$$\begin{aligned} &\Theta_\nu \rightharpoonup \Theta \qquad \text{weakly in } L^p(0,1) \\ \text{that is} \qquad &\int \Theta_\nu \psi \,\mathrm{d}x \to \int \Theta \psi \,\mathrm{d}x \qquad \text{for } \psi \in L^{p'}(0,1) \end{aligned} \tag{5.35}$$

with $p'$ the dual exponent of $p$. Setting $\psi(y) = \chi_{[0,x]}(y)$, the characteristic function of $[0, x]$, we deduce

$$G_\nu(x) = \int_0^x \Theta_\nu(s)\mathrm{d}s \to G(x) := \int_0^x \Theta(s)\,\mathrm{d}s \tag{5.36}$$

Next, we employ ideas developed in the context of zero-viscosity limits for Riemann problems of conservation laws (Tzavaras 1994, 1996; Papadoperakis 1999). We set

$$\pi_\nu := \frac{\mathrm{d}\, V_\nu}{\mathrm{d}x} = V_\infty \, \frac{e^{\frac{1}{\nu}G_\nu(x)}}{\int_0^1 e^{\frac{1}{\nu}G_\nu(t)}\mathrm{d}t}, \tag{5.37}$$

where $G_\nu(x) = \displaystyle\int_0^x \Theta_\nu(s)\,\mathrm{d}s$ and view $\{\pi_\nu\}$ as a sequence of probability measures. By (5.37), the sequence $\{\pi_\nu\}$ is uniformly bounded in measures and there exists a subsequence $\pi_\nu$ and a probability measure $\pi$ such that

$$\pi_\nu \overset{*}{\rightharpoonup} \pi, \quad \text{in measures} \quad \mathcal{M}[0,1]. \tag{5.38}$$

Due to the correspondence between functions of bounded variations and Borel measures (Folland 2013, Sec 3.5, Sec 7.3) one sees that the distribution function of the measure $\pi$ is precisely the function $V(x+)$ and (5.38) reflects (5.34).

We are now ready to state the first convergence theorem.

**Theorem 5.4** *Assume that $E_0 + \frac{1}{2}V_\infty^2 > 0$ and let $\{(\Theta_\nu, V_\nu)\}_{\nu>0}$ be a family of solutions satisfying the uniform bound (B). There exists a subsequence and a function $(\Theta, V)$ such that*

$$V_\nu \to V, \quad a.e.\ x \in (0,1), \qquad \Theta_\nu \rightharpoonup \Theta \ \ wk\text{-}L^p(0,1) \text{ with } 1 \le p < 2,$$

*and $(\Theta, V)$ satisfies*

(i) *either $\operatorname{supp}\pi = [0, a]$, $a > 0$, in which case $\Theta = 0$ on $[0, a]$, while $V = Y(x)$ for $x \in [0, a]$, $V = V_\infty$ for $x \in [a, 1]$ where $Y(x)$ is some nondecreasing function;*

(ii) *or $\operatorname{supp}\pi = \{0\}$ and $V = 0$ for $x = 0$, while $V = V_\infty$ for $x \in (0, 1]$.*

*In either case $(V, \Theta)$ satisfy the differential inequality*

$$\frac{1}{2}\Theta^2(x) \le \frac{x}{(1-x^2)^2}\Big(H(V;x) + E_0\,(1-x)\Big) \tag{5.39}$$

*in the sense of distributions where $H(V;x)$ is given by (5.31).*

***Proof*** For any subset $[0,\alpha] \subset [0,1)$, the Ascoli–Arzela theorem with hypothesis (B) implies that along a subsequence $G_\nu$ converges uniformly on $[0,\alpha] \subset [0,1)$. In particular,

$$G_\nu(x) \to G(x) = \int_0^x \Theta(s)\,\mathrm{d}s \tag{5.40}$$

uniformly on any compact $[0,\alpha] \subset [0,1)$ and pointwise on $(0,1)$ as indicated in (5.36). The limit $G$ is continuous on $[0,1)$.

We proceed to study the $\operatorname{supp}\pi$. To this end, define

$$S = \{x \in [0,1) : G(x) = \max_{y\in[0,1)} G(y) = 0\}, \tag{5.41}$$

The function $G$ is nonincreasing, $G(0) = 0$, and $S$ the set of point where $G$ attains its maximum.

**Lemma 5.5** *Let $\pi$ be the weak-$*$ limit of $\pi_\nu$ defined in (5.37). Then, $\operatorname{supp}\pi \subset S$.*

***Proof*** Let $x_0 \in S$ be fixed and suppose there exists $x_1 \in [0,1)$ such that $x_1 \notin S$. Then,

$$G(x_1) < G(x_0) = \max_{y\in[0,1)} G(y).$$

Since $G$ is nonincreasing and continuous, there exists $\delta > 0$ such that for $x \in [x_0 - \delta, x_0 + \delta]$ and $y \in [x_1 - \delta, x_1 + \delta]$

$$G(y) \le \max_{z\in[x_1-\delta,x_1+\delta]} G(z) < \min_{z\in[x_0-\delta,x_0+\delta]} G(z) \le G(x). \tag{5.42}$$

Setting $d_M := \max_{z\in[x_1-\delta,x_1+\delta]} G(z)$, $D_m := \min_{z\in[x_0-\delta,x_0+\delta]} G(z)$, we have by (5.42) that $d_M < D_m$ and we fix $\eta$ such that

$$0 < \eta < \frac{D_m - d_M}{4}.$$

Define $J = [x_0 - \delta, x_0 + \delta] \cup [x_1 - \delta, x_1 + \delta] \subset [0,1)$ and select $\delta$ small so that $J \subset [0,1)$. Since $G_\nu \to G$ uniformly on $J$ there exist $\nu_0 > 0$ such that for any $\nu < \nu_0$

$$G_\nu(y) \le G(y) + \eta \le d_M + \eta < D_m - \eta \le G(x) - \eta \le G_\nu(x), \tag{5.43}$$

for $x \in [x_0 - \delta, x_0 + \delta]$ and $y \in [x_1 - \delta, x_1 + \delta]$. Now,

$$\pi_\nu([x_1 - \delta, x_1 + \delta]) = \int_{[x_1-\delta,x_1+\delta]} \pi_\nu(\mathrm{d}x) = V_\infty \frac{\int_{[x_1-\delta,x_1+\delta]} e^{\frac{1}{\nu}G_\nu(t)}\mathrm{d}t}{\int_0^1 e^{\frac{1}{\nu}G_\nu(t)}\mathrm{d}t},$$

$$\leq V_\infty \frac{\int_{[x_1-\delta,x_1+\delta]} e^{\frac{1}{\nu}G_\nu(t)}\mathrm{d}t}{\int_{[x_0-\delta,x_0+\delta]} e^{\frac{1}{\nu}G_\nu(t)}\mathrm{d}t}.$$

From (5.43), it follows

$$\pi_\nu([x_1-\delta,x_1+\delta]) \leq V_\infty\, e^{-\frac{1}{\nu}(D_m-d_M-2\eta)} \to 0, \quad \text{as } \nu \to 0.$$

Hence, $\pi([x_1-\delta,x_1+\delta]) = 0$ and $x_1 \notin \operatorname{supp}\pi$. □

The special structure of our problem induces a structural property on the support of $\pi$.

**Lemma 5.6** *Let $\operatorname{supp}\pi \neq \emptyset$. If $\bar{x} > 0$ satisfies $\bar{x} \in supp\ \pi$, then for any $0 < x_0 < \bar{x}$ we have $x_0 \in supp\ \pi$.*

***Proof*** Let $\bar{x} \in supp\ \pi$, $\bar{x} > 0$. Then, for any $\delta > 0$ we have $\pi\big([\bar{x}-\delta,\bar{x}+\delta]\big) > 0$. We will prove that if $0 < x_0 < \bar{x}$ and $\delta$ as above then

$$\pi\big([x_0-\delta,x_0+\delta]\big) > 0. \tag{5.44}$$

In turn, that implies $x_0 \in \operatorname{supp}\pi$.

Using (5.37), we have

$$0 < \pi_\nu([\bar{x}-\delta,\bar{x}+\delta]) = V_\infty \frac{\int_{[\bar{x}-\delta,\bar{x}+\delta]} e^{\frac{1}{\nu}G_\nu(t)}dt}{\int_0^1 e^{\frac{1}{\nu}G_\nu(t)}\mathrm{d}t}.$$

Recall that $G_\nu$ is nonincreasing. Using the change of variables $t = y + \tau$ with $\tau = \bar{x} - x_0 > 0$, in the top integral implies

$$\int_{[\bar{x}-\delta,\bar{x}+\delta]} e^{\frac{1}{\nu}G_\nu(t)}\mathrm{d}t = \int_{[x_0-\delta,x_0+\delta]} e^{\frac{1}{\nu}G_\nu(\tau+y)}\mathrm{d}y \leq \int_{[x_0-\delta,x_0+\delta]} e^{\frac{1}{\nu}G_\nu(y)}\mathrm{d}y$$

Therefore,

$$\pi_\nu([\bar{x}-\delta,\bar{x}+\delta]) \leq \pi_\nu([x_0-\delta,x_0+\delta]).$$

Letting $\nu \to 0$, we conclude

$$0 < \pi([\bar{x}-\delta,\bar{x}+\delta]) \leq \pi([x_0-\delta,x_0+\delta]).$$

which shows (5.44). □

Since $0 = V(0) < V(1) = V_\infty$ we have that $\operatorname{supp}\pi \neq \emptyset$. Moreover, the form of $G(x)$ leads to the following lemma.

**Lemma 5.7** *Suppose there exists $\bar{x} > 0$ such that $\bar{x} \in supp\,\pi$. Then,*

$$\Theta(x) = 0 \quad \textit{for a.e.} \quad x \in supp\,\pi. \tag{5.45}$$

***Proof*** Since $\Theta \in L^1(0,1)$, the Lebesgue differentiation theorem implies

$$\lim_{\substack{|I|\to 0 \\ \bar{x}\in I}} \frac{1}{|I|}\int_I \Theta(s)\,\mathrm{d}s = \Theta(x) \quad a.e.,$$

where $I$ is any interval containing $x$. If $\bar{x} \in \operatorname{supp}\pi \subset S$ then

$$\lim_{\substack{h\to 0 \\ h>0}} \frac{1}{h}\int_{\bar{x}}^{\bar{x}+h} \Theta(s)\,\mathrm{d}s = \lim_{\substack{h\to 0 \\ h>0}} \frac{1}{h}\Big(G(\bar{x}+h) - G(\bar{x})\Big) \le 0,$$
$$\lim_{\substack{h\to 0 \\ h<0}} \frac{1}{h}\int_{\bar{x}-h}^{\bar{x}} \Theta(s)\,\mathrm{d}s = \lim_{\substack{h\to 0 \\ h>0}} \frac{1}{h}\Big(G(\bar{x}) - G(\bar{x}-h)\Big) \ge 0.$$

Hence it follows that $\Theta(\bar{x}) = 0 \quad a.e.$ □

By virtue of Lemma 5.6 and the fact that $\operatorname{supp}\pi \neq \emptyset$ there are two possibilities: either (i) $\operatorname{supp}\pi = [0, a]$ for some $a > 0$, or (ii) $\operatorname{supp}\pi = \{0\}$. In either case

$$\operatorname{supp}\pi \subset S = \{x \in [0,1) : G(x) = 0\}, \qquad \Theta(x) = 0 \quad \text{for a.e. } x \in \operatorname{supp}\pi.$$

We conclude:

**Case 1:** $\operatorname{supp}\pi = [0, a]$ with $a > 0$. Then $\Theta(x) = 0$ on $[0, a]$ and

$$V(x) = \begin{cases} Y(x) & x \in [0, a] \\ V_\infty, & x \in [a, 1) \end{cases} \tag{5.46}$$

for some nondecreasing function $Y(x)$.

**Case 2:** $\operatorname{supp}\pi = \{0\}$ and

$$V(x) = \begin{cases} 0 & x = 0 \\ V_\infty, & x \in (0, 1) \end{cases} \tag{5.47}$$

This provides some information on $(V, \Theta)$, but it is incomplete. Some further information is obtained by passing to the limit $\nu \to 0$ in (5.19). First, the convergence (5.34) implies

$$H(V_\nu; x) \to H(V; x) = \left[\int_x^1 \frac{1-t^2}{t^2}\left(\int_0^t \frac{\sigma}{(1-\sigma^2)^2} V^2(\sigma)d\sigma\right)\mathrm{d}t\right]$$

Then (5.19) together with the property that $\Theta(x)^2 \leq \text{wk-lim}(\Theta_n(x)^2)$ imply that $(\Theta, V)$ satisfy the differential inequality

$$\frac{1}{2}\Theta^2(x) \leq \frac{x}{(1-x^2)^2}\Big(H(V;x) + E_0\ (1-x)\Big) \tag{5.48}$$

in the sense of distributions. □

The inequality (5.39) is due to the fact that only weak convergence for $\Theta$ is available under (B). It can be improved if we have pointwise convergence for $\Theta$, namely if

$$\Theta_\nu \to \Theta \quad a.e., \ as \quad \nu \to 0. \tag{A}$$

We will later justify (A) under the hypothesis $E_0 > 0$. Using (A), one may pass to the limit in (5.19) in the sense of distributions and deduce

$$\frac{\Theta^2(x)}{2} = \mathcal{F}(V, x). \tag{5.49}$$

Let us compute $\Theta(x)$ for Case 2. Since $V(x)$ is given by (5.47), (5.49) yields

$$\frac{\Theta^2(x)}{2} = \mathcal{F}(V_\infty, x) = \big(\frac{1}{2}V_\infty^2 + E_0\big)\ \frac{x(1-x)}{(1-x^2)^2}$$

and thus, since $\Theta(x) < 0$,

$$\Theta(x) = -\sqrt{V_\infty + 2E_0}\ \frac{\sqrt{x(1-x)}}{(1-x^2)}.$$

For Case 1, we recall that $V(x)$ is given by (5.46) and $\Theta(x) = 0$ a.e. for $x \in [0, a]$, $a > 0$. Then (5.49) with (5.17) implies

$$E_0\ (1-x) = -\int_x^1 \frac{1-t^2}{t^2}\Big(\int_0^t \frac{\sigma}{(1-\sigma^2)^2} V^2(\sigma)\mathrm{d}\sigma\Big)\,\mathrm{d}t\,, \quad \text{for } x \in [0, a].$$

If we differentiate this, we get

$$E_0\ \frac{x^2}{1-x^2} = -\int_0^x \frac{\sigma}{(1-\sigma^2)^2} V^2(\sigma)\mathrm{d}\sigma.$$

Differentiating once more yields

$$V^2(x) = -2\ E_0 \quad for\ x \in (0, a)\,,$$

which contradicts the assumption $\operatorname{supp}\pi = [0, a]$ with $a > 0$. We conclude that only Case 2 can happen and $(\Theta_\nu, V_\nu)$ converges almost everywhere as $\nu \to 0$ to a solution $(\Theta, V)$ of the Euler equations. This provides a criterion to select the type of

Euler solution that occurs and clearly only solutions with solutions with $\Theta < 0$ are admissible.

In conclusion, we have the following theorem

**Theorem 5.8** *Assume that* $E_0 + \frac{1}{2}V_\infty^2 > 0$ *and* $\{(\Theta_\nu, V_\nu)\}_{\nu>0}$ *is a family of solutions satisfying the uniform bound* (B) *and the convergence* (A). *Then* $(\Theta, V)$ *is a smooth solution of* (2.14) *with the form described in Sect.* 3, *but under the restriction* $\Theta(x) < 0$.

If the solution takes values in the range where $\Theta(x) < 0$ then it lies in Zone A. The analysis of Sect. 5.3 shows that $F$ in (5.26) then takes values $F(x) > 0$ on $(0, 1)$. The reader should note that numerical computations suggest that as $\nu$ decreases the solution of (5.16) enters Zone A, that is the region that $\Theta(x) < 0$, and stays there. No oscillations in $\Theta$ are observed numerically.

We next restrict in the range $E_0 > 0$ and justify (A).

**Proposition 5.9** *If* $E_0 > 0$ *then the family of function* $\{A_\nu(x)\}$ *defined by*

$$A_\nu(x) = (1 - x^2)\Theta_\nu(x) \tag{5.50}$$

*is of bounded variation on* $[0, 1]$ *and along a subsequence* $\{\Theta_\nu\}$ *satisfies (A).*

***Proof*** Using (5.19) we see that the functions $\{A_\nu\}$ in (5.50) satisfy the differential equation

$$\nu(1 - x^2)\frac{\mathrm{d}A_\nu}{\mathrm{d}x} = \tfrac{1}{2}A_\nu^2 - 2x\nu A_\nu - R(x) \tag{5.51}$$

where

$$R(x) := xF(x) = x\Big(H(x) + E_0(1 - x)\Big) \tag{5.52}$$

Observe that $A(0) = 0$ and using (5.13), (5.15), (5.11) and the L'Hopital rule we compute

$$A(1) = \lim_{x\to 1}(1 - x^2)\Theta(x) = \lim_{\xi\to\infty}\frac{\hat{\theta}(\xi)}{1 + \xi^2} = \lim_{\xi\to\infty}\frac{\theta(\xi)}{\sqrt{1 + \xi^2}} = \theta'(\infty) = 0$$

The uniform bounds (B) imply

$$-\sqrt{\kappa}\sqrt{x(1 - x)} \le A_\nu(x) < 0 \tag{5.53}$$

Next, turn to (5.52) and use the hypothesis $E_0 > 0$ together with (5.21), (5.22) to conclude that

$$R(x) > 0, \quad \frac{\mathrm{d}^2R}{\mathrm{d}x^2} = x\frac{\mathrm{d}^2H}{\mathrm{d}x^2} + 2x\Big(\frac{\mathrm{d}H}{\mathrm{d}x} - E_0\Big) < 0 \quad x \in (0, 1) \tag{5.54}$$

$\frac{dR}{dx}(0) = H(0) + E_0 > 0$, $\frac{dR}{dx}(1) = \frac{dH}{dx}(1) - E_0 < 0$. We see that $R(x)$ has a concave graph, vanishing at the endpoints, facing downwards.

Since $A(0) = A(1) = 0$ the function $A(x)$ must have at least one minimum, that is by the nature of the boundary condition the function $A(x)$ oscillates once. Again due to the boundary conditions it must have an odd number of oscillations. By Sard's theorem the set of critical values of $A$ has measure zero. If the graph of $A$ has three oscillations, then there will be a level $c < 0$—which can be selected so as not to be a critical value—and four consecutive points $x_1 < x_2 < x_2 < x_4$ such that $A(x_1) = A(x_2) = A(x_3) = A(x_4) = c$, while $\frac{dA}{dx}(x_1) < 0$, $\frac{dA}{dx}(x_2) > 0$, $\frac{dA}{dx}(x_3) < 0$ and $\frac{dA}{dx}(x_4) > 0$.

The function $f(x) := \frac{1}{2}c^2 - 2\nu x c - R(x)$ satisfies

$$f(x_1) > 0, \quad f(x_2) < 0, \quad f(x_3) > 0, \quad f(x_4) < 0.$$

Then, there are three consecutive points $y_1 < y_2 < y_3$ in $(0, 1)$ where the function $f$ vanishes. This contradicts the fact that by (5.54) the function $f$ is strictly convex.

We conclude that $A(x)$ is initially decreasing, reaches a minimum and is afterwards increasing. It also satisfies (5.53). Hence $\{A_\nu\}_{\nu>0}$ has uniformly bounded total variation and along a subsequence $A_\nu(x) \to A(x)$ for almost every $x \in (0, 1)$. Obviously $A_\nu \rightharpoonup A$ weakly and we conclude using (5.35) that $A = (1 - x^2)\Theta$ and (A) holds. □

Combining Proposition 5.9 with Theorem 5.8 gives

**Corollary 5.10** *If $E_0 > 0$ then the family of solutions $\{(\Theta_\nu, V_\nu)\}_{\nu>0}$ is of bounded variation and along a subsequence converges, $\Theta_\nu \to \Theta$ and $V_\nu \to V$ a.e. in $(0, 1)$. The function $(\Theta, V)$ is a smooth solution of (2.14) of the form described in Sect. 3, and satisfies the restriction $\Theta(x) < 0$.*

Note that when $V_\infty > 0$ among the two solutions of the Euler equations (3.10) the one selected at the zero-viscosity limit corresponds to the negative sign, see Fig. 2b. One easily checks that when $V_\infty < 0$ again the negative sign is selected.

## 6 Boundary Layer Analysis for a Model Problem

In this section, we investigate the asymptotic behaviour of solutions of system (5.16) as $\nu \to 0$. We consider a model problem which is a simplification of the initial equations, with the objective to understand the boundary layer. For small viscosities, $V(x)$ is approximated by setting $V(x) \equiv V_\infty$, leading to

$$\mathcal{F}(V, x) = \mathcal{F}(V_\infty, x) = \Big(\frac{V_\infty^2}{2} + E_0\Big)\frac{x - x^2}{(1 - x^2)^2}.$$

This reduces system (5.16) to a simpler form which will be referred to as the model problem, namely,

$$\frac{\bar{\Theta}^2(x)}{2} - \nu\frac{d\bar{\Theta}}{dx}(x) = K\frac{x - x^2}{(1 - x^2)^2}, \tag{6.1a}$$

$$\nu \frac{\mathrm{d}^2 \bar{V}}{\mathrm{d}^2 x} = \bar{\Theta}\ \frac{\mathrm{d}\bar{V}}{\mathrm{d}x}, \tag{6.1b}$$

$$\bar{\Theta}(0) = 0, \quad \bar{V}(0) = 0, \quad \bar{V}(1) = V_\infty, \tag{6.1c}$$

where $K = \frac{V_\infty^2}{2} + E_0 > 0$. Note that equation (6.1a) for $\bar{\Theta}$ is now independent of $\bar{V}$, while (6.1b) is still coupled.

We use the method of matched asymptotic expansions from singular perturbation theory. The method aims to construct an asymptotic approximation of the solution inside the boundary layer and a solution valid away from the boundary layer, and then combine them through a matching process. We refer to solutions within the boundary layer as inner solutions and to solutions away of the layer as the outer solutions, Lagerstrom (1988), Holmes (2013).

We consider first the equation (6.1a) for $\bar{\Theta}$

$$\frac{\bar{\Theta}^2(x)}{2} - \nu \frac{\mathrm{d}\bar{\Theta}}{\mathrm{d}x}(x) = K \frac{x - x^2}{(1 - x^2)^2}, \tag{6.2a}$$

$$\bar{\Theta}(0) = 0, \tag{6.2b}$$

and apply the method of matched asymptotic expansions. To construct the outer solution, assume that $\bar{\Theta}$ can be written as a power series with powers of $\nu$,

$$\bar{\Theta}(x) \approx \bar{\Theta}_0(x) + \nu \bar{\Theta}_1(x) + \mathcal{O}(\nu^2),$$

and substitute it back to (6.2a). If we focus on the leading terms, i.e. terms of order $\nu^0$, we obtain the equation

$$\bar{\Theta}_0(x) = \pm \sqrt{2\, K \frac{x - x^2}{(1 - x^2)^2}}. \tag{6.3}$$

The choice for the sign $\bar{\Theta}_0$ will depend on $\bar{\Theta}$. Recall that $\bar{\Theta}$ solve the equation (6.2a), we have

$$\bar{\Theta}(0) = 0, \quad \frac{\mathrm{d}\bar{\Theta}}{\mathrm{d}x}(0) = 0, \quad \text{and} \quad \frac{\mathrm{d}^2\bar{\Theta}}{\mathrm{d}x^2}(0) < 0,$$

which implies $\bar{\Theta}$ should be negative for all $0 < x < 1$. Hence, we choose $\bar{\Theta}_0$ to be negative. Note that the boundary condition at $x = 0$ is automatically satisfied.

We proceed now with the inner solution. Expecting the boundary layer to locate at $x = 0$, we introduce the stretched variable $\eta = \nu^{-\frac{2}{3}} x$. Setting $\Phi(\eta) = \nu^{-\frac{1}{3}} \bar{\Theta}(x)$, the problem (6.2a)–(6.2b) takes the form

$$\frac{\Phi^2}{2} - \frac{\mathrm{d}\Phi}{\mathrm{d}\eta} = K \frac{\eta}{(1 - \nu^{\frac{2}{3}}\, \eta)(1 + \nu^{\frac{2}{3}}\, \eta)^2} \tag{6.4a}$$

$$\Phi(0) = 0, \tag{6.4b}$$

If the approximation of $\Phi$ in powers of $\nu$ is given by

$$\Phi(\eta) \approx \Phi_0(\eta) + \nu\Phi_1(\eta) + \mathcal{O}(\nu^2),$$

and using the Taylor expansion of the right-hand side of (6.4a),

$$\frac{\eta}{(1-\nu^{\frac{2}{3}}\eta)(1+\nu^{\frac{2}{3}}\eta)^2} \approx \eta + \mathcal{O}(\nu^{\frac{2}{3}}),$$

we obtain for the leading term

$$\frac{\Phi_0^2}{2} - \frac{\mathrm{d}\Phi_0}{\mathrm{d}\eta} = K\,\eta, \tag{6.5a}$$

$$\Phi_0(0) = 0. \tag{6.5b}$$

Inspired by Holmes and Stein (1976), equation (6.5a) can be transformed into the well-known Airy equation

$$y''(t) - t\,y(t) = 0.$$

Using the transformation

$$\Phi_0(\eta) = -\frac{2}{\mathcal{U}(\eta)}\frac{\mathrm{d}\mathcal{U}}{\mathrm{d}\eta}, \tag{6.6}$$

equation (6.5a) reduces to

$$\frac{\mathrm{d}^2\mathcal{U}}{\mathrm{d}\eta^2} = \frac{K}{2}\eta\,\mathcal{U}(\eta).$$

and its solutions are given as a linear combination of special functions $Ai$, the Airy function of the first kind, and $Bi$, the Airy function of the second kind, see (Holmes 2013, Appendix B.1). Namely,

$$\mathcal{U}(\eta) = \mathrm{Ai}\left(\left(\frac{K}{2}\right)^{1/3}\eta\right)c_1 + \mathrm{Bi}\left(\left(\frac{K}{2}\right)^{1/3}\eta\right)c_2,$$

where $c_1, c_2$ are integration constants. Using (6.6), we express $\Phi_0$ as a linear combination of Airy functions $Ai$, $Bi$ and their derivatives $Ai'$, $Bi'$. Hence, $\Phi_0$ takes the form

$$\Phi_0(\eta) = -2\left(\frac{K}{2}\right)^{1/3}\frac{\mathrm{Ai}'\left(\left(\frac{K}{2}\right)^{1/3}\eta\right)c_1 + \mathrm{Bi}'\left(\left(\frac{K}{2}\right)^{1/3}\eta\right)c_2}{\mathrm{Ai}\left(\left(\frac{K}{2}\right)^{1/3}\eta\right)c_1 + \mathrm{Bi}\left(\left(\frac{K}{2}\right)^{1/3}\eta\right)c_2},$$

or equivalently,

$$\Phi_0(\eta) = -2\left(\frac{K}{2}\right)^{1/3} \frac{\mathrm{Ai}'\left(\left(\frac{K}{2}\right)^{1/3}\eta\right) C + \mathrm{Bi}'\left(\left(\frac{K}{2}\right)^{1/3}\eta\right)}{\mathrm{Ai}\left(\left(\frac{K}{2}\right)^{1/3}\eta\right) C + \mathrm{Bi}\left(\left(\frac{K}{2}\right)^{1/3}\eta\right)},$$

where $C = \frac{c_1}{c_2}$ is a constant. Imposing now the boundary condition (6.5b), we get

$$0 = \frac{\mathrm{Ai}'(0)\, C + \mathrm{Bi}'(0)}{\mathrm{Ai}(0)\, C + \mathrm{Bi}(0)} = \frac{-\frac{C}{3^{1/3}\,\Gamma\left(\frac{1}{3}\right)} + \frac{3^{1/6}}{\Gamma\left(\frac{1}{3}\right)}}{\frac{C}{3^{2/3}\Gamma\left(\frac{2}{3}\right)} + \frac{1}{3^{1/6}\Gamma\left(\frac{2}{3}\right)}} = \frac{3^{1/3}\,\Gamma(\frac{2}{3})(-C+\sqrt{3})}{\Gamma(\frac{1}{3})(C+\sqrt{3})},$$

where $\Gamma$ denotes the Gamma function. Thus, the constant $C$ is determined as

$$C = \sqrt{3}.$$

Consequently, the leading term $\Phi_0$ of the inner solution becomes

$$\Phi_0(\eta) = -2\left(\frac{K}{2}\right)^{1/3} \frac{\sqrt{3}\,\mathrm{Ai}'\left(\left(\frac{K}{2}\right)^{1/3}\eta\right) + \mathrm{Bi}'\left(\left(\frac{K}{2}\right)^{1/3}\eta\right)}{\sqrt{3}\,\mathrm{Ai}\left(\left(\frac{K}{2}\right)^{1/3}\eta\right) + \mathrm{Bi}\left(\left(\frac{K}{2}\right)^{1/3}\eta\right)}.$$

The last step of the method of matched asymptotic expansions is to derive a uniform expansion of the solution of (6.2a) over the whole domain $[0, 1)$. Combining the approximations of inner and outer solution, we conclude that the asymptotic expansion of $\bar{\Theta}$ as $\nu \to 0$ is

$$\bar{\Theta}(x) \approx \begin{cases} -\sqrt{2\,K\,\dfrac{x-x^2}{(1-x^2)^2}}, & A\nu^{\frac{2}{3}} < x < 1 \\ \Phi_0(\nu^{-\frac{2}{3}}\,x), & 0 \le x \le A\nu^{\frac{2}{3}} \end{cases} \tag{6.7}$$

where $A$ is a positive constant and

$$\Phi_0(\nu^{-\frac{2}{3}}\,x) = -2\nu^{1/3}\left(\frac{K}{2}\right)^{1/3} \frac{\sqrt{3}\mathrm{Ai}'\left(\left(\frac{K}{2}\right)^{1/3}\nu^{-\frac{2}{3}}\,x\right) + \mathrm{Bi}'\left(\left(\frac{K}{2}\right)^{1/3}\nu^{-\frac{2}{3}}\,x\right)}{\sqrt{3}\mathrm{Ai}\left(\left(\frac{K}{2}\right)^{1/3}\nu^{-\frac{2}{3}}\,x\right) + \mathrm{Bi}\left(\left(\frac{K}{2}\right)^{1/3}\nu^{-\frac{2}{3}}\,x\right)}.$$

Moreover, the boundary layer is formed at $x = 0$ and its size is of order $\nu^{\frac{2}{3}}$.

Let us consider now the equation (6.1b) for $\bar{V}$. Motivated by the asymptotic expansion of $\bar{\Theta}$, we introduce the following simplified problem

$$\nu\frac{\mathrm{d}^2\bar{V}}{v^2x}(x) = -\sqrt{2\,K\,\frac{x-x^2}{(1-x^2)^2}}\,\frac{\mathrm{d}\bar{V}}{\mathrm{d}x}(x), \tag{6.8a}$$

$$\bar{V}(0) = 0, \quad \bar{V}(1) = V_\infty, \tag{6.8b}$$

and apply the method of matched asymptotic expansions. As before, we expect the boundary layer to be located at $x = 0$.

First, we derive the approximation of the outer solution. Assuming that $\bar{V}$ can be expressed as a power series with powers of $\nu$, i.e.

$$\bar{V}(x) \approx \bar{V}_0(x) + \nu \bar{V}_1(x) + \mathcal{O}(\nu^2),$$

the equation (6.8a) yields the following differential equation for the lead term $\bar{V}_0$

$$-\sqrt{2\,K\,\frac{x-x^2}{(1-x^2)^2}}\,\frac{\mathrm{d}\bar{V}_0}{\mathrm{d}x} = 0 \quad \text{which implies} \quad \bar{V}_0(x) \equiv c, \tag{6.9}$$

where $c$ is a constant. To determine this constant, we consider the boundary condition away from the boundary layer, i.e. at $x = 1$ and thus, (6.8b) implies

$$\bar{V}_0(x) \equiv V_\infty. \tag{6.10}$$

For the inner solution we introduce the variable $\eta = \nu^{-2/3}\,x$ and set $\bar{V}(x) = Y(\eta)$. The problem (6.8) reduces to

$$\frac{\mathrm{d}^2 Y}{\mathrm{d}^2\eta} + \sqrt{2\,K}\,\sqrt{\frac{\eta}{(1-\nu^{\frac{2}{3}}\,\eta)(1+\nu^{\frac{2}{3}}\,\eta)^2}}\,\frac{\mathrm{d}Y}{\mathrm{d}\eta} = 0 \quad \text{with} \quad Y(0) = 0. \tag{6.11}$$

If the approximation of $Y$ in powers of $\nu$ is expressed as

$$Y(\eta) \approx Y_0(\eta) + \nu Y_1(\eta) + \mathcal{O}(\nu^2),$$

and the Taylor expansion of the right-hand side of (6.11) is

$$\sqrt{\frac{\eta}{(1-\nu^{\frac{2}{3}}\,\eta)(1+\nu^{\frac{2}{3}}\,\eta)^2}} \approx \sqrt{\eta} + \mathcal{O}(\nu^{\frac{2}{3}}),$$

then we have to solve the following problem for leading-order term $Y_0$

$$\begin{aligned} \frac{\mathrm{d}^2 Y_0}{\mathrm{d}^2\eta} + \sqrt{2\,K\,\eta}\,\frac{\mathrm{d}Y_0}{\mathrm{d}\eta} &= 0, \\ Y_0(0) &= 0. \end{aligned}$$

Its solution is

$$Y_0(\eta) = C \int_0^\eta e^{-\frac{2\sqrt{2\,K}}{3}\,s^{3/2}}\,\mathrm{d}s,$$

where $C$ is an integration constant. Since both boundary conditions (6.8b) have been taken into consideration, the unknown $C$ is determined by matching the outer and the inner expansions. Considering that both the inner and outer solutions approximate the same function in different regions, we impose that the two solutions are equal in a transition area close to the boundary layer, Holmes (2013). Therefore, we require

$$\lim_{x\to 0} \bar{V}_0(x) = \lim_{\eta\to\infty} Y_0(\eta),$$

that implies

$$C = \frac{V_\infty}{\int_0^\infty e^{-\frac{2\sqrt{2K}}{3} s^{3/2}} \mathrm{d}s},$$

and completes the derivation of the inner solution.

As the last step of the method of matched asymptotic expansions, we derive a uniform expansion of the solution of (6.8) over the whole domain $[0, 1)$. Therefore, as $\nu \to 0$ the asymptotic expansion of $\bar{V}(x)$ takes the form

$$\bar{V}(x) \approx V_\infty \frac{\int_0^{\nu^{-2/3}x} e^{-\frac{2\sqrt{2K}}{3} s^{3/2}} ds}{\int_0^\infty e^{-\frac{2\sqrt{2K}}{3} s^{3/2}} ds} + \mathcal{O}(\nu). \tag{6.12}$$

and the boundary layer at $x = 0$ is of the same size as for $\bar{\Theta}(x)$.

## 7 Stationary Navier–Stokes—Numerical Results

In this section we construct a numerical scheme to solve the coupled system of ordinary differential equations (5.9) using an iterative algorithm. Moreover, we illustrate some numerical experiments for different values of the parameters $\nu$, $E_0$ and $V_\infty$.

Let us recall the system (5.9). For convenience we use the equivalent formulation of the problem, system (5.16a)–(5.16d) in variable $x$, where $0 < x < 1$

$$\frac{\Theta^2(x)}{2} - \nu \frac{\mathrm{d}\Theta}{\mathrm{d}x}(x) = \mathcal{F}(V, x), \tag{7.1a}$$

$$\nu \frac{\mathrm{d}^2 V}{\mathrm{d}^2 x}(x) = \Theta(x) \frac{\mathrm{d}V}{\mathrm{d}x}(x), \tag{7.1b}$$

equipped with the boundary conditions

$$\Theta = V = 0, \quad \text{at} \quad x = 0, \tag{7.2a}$$

$$V \to V_\infty, \quad \text{as} \quad x \to 1, \tag{7.2b}$$

where the functional $\mathcal{F}(V, x)$ is defined by

$$\mathcal{F}(x) = \mathcal{F}(V, x; E_0) = \frac{x}{(1-x^2)^2}\left[\int_x^1 \frac{1-t^2}{t^2}\left(\int_0^t \frac{\sigma}{(1-\sigma^2)^2} V^2(\sigma) d\sigma\right) \mathrm{d}t + E_0\,(1-x)\right]. \quad (7.3)$$

### 7.1 Discretization

To obtain numerical approximations to system (7.1a)–(7.2b) we use an iterative algorithm: Given $V$ we solve numerically the initial value problem (7.1a) by a Runge–Kutta method and update $\Theta$ which is then used to solve the two-point boundary value problem (7.1b) using finite differences. This process is repeated until convergence. The algorithm is described in detail in Sect. 7.2.

The discretization of (7.1b) is based on finite differences. On $[0, 1]$ we introduce a uniform mesh of fixed width $\Delta x$. Given $N \in \mathbb{N}$, set $\Delta x = \frac{1}{N}$ and define the discrete points $x_j = j\Delta x$, $j = 0, 1, 2, \ldots, N$. We denote by $\Theta^j \approx \Theta(x_j)$ and $V^j \approx V(x_j)$ and use central finite differences to discretize (7.1b) and obtain

$$\nu \frac{V^{j+1} - 2V^j + V^{j-1}}{\Delta x^2} = \Theta^j \frac{V^{j+1} - V^{j-1}}{2\Delta x}, \quad j = 1, \ldots, N-1, \qquad V^0 = 0,\ V^N = V_\infty, \quad (7.4)$$

or equivalently

$$V^{j-1}\left(2\nu + \Delta x\,\Theta^j\right) - 4\nu\, V^j + V^{j+1}\left(2\nu - \Delta x\,\Theta^j\right) = 0, \qquad j = 1, \ldots, N-1, \qquad V^0 = 0,\ V^N = V_\infty, \quad (7.5)$$

which forms a tri-diagonal linear system solved by a direct method.

To discretize the nonlinear initial value problem (7.1a) we use a Runge–Kutta method. The Runge–Kutta methods are multistage methods that compute approximations to the solution at intermediate points which are later combined to advance the solution at the next discretization point. Equation (7.1a) can be rewritten as

$$\nu \frac{\mathrm{d}\Theta}{\mathrm{d}x}(x) = \frac{\Theta^2(x)}{2} - \mathcal{F}(x). \quad (7.6)$$

For simplification of the presentation, we denote the right-hand side of the above relation as follows $f(x, V, \Theta) = \frac{1}{2}\Theta^2 - \mathcal{F}(x)$. The Runge–Kutta method for (7.1a) is obtained by discretizing the derivative using the following method:

1. Set $\Theta^{j,1} = \Theta^j$, where $\Theta^j$ is the approximate solution at grid point $x_j$.

2. Compute the $\mathcal{K}$ intermediate stages for $m = 1, \ldots, \mathcal{K}$

$$\nu\Theta^{j,m} = \nu\Theta^{j} + \Delta x \sum_{s=1}^{\mathcal{K}} \alpha_{m,s} f\left(x_j + c_s \Delta x, V^{j,s}, \Theta^{j,s}\right), \tag{7.7}$$

where $V^{j,s} \approx V(x_j + c_s\Delta x)$ and $\Theta^{j,s} \approx \Theta(x_j + c_s\Delta x)$. The coefficients $\alpha_{m,s}$ are constants with sum for every row equals to $c_m$, i.e.

$$\sum_{s=1}^{\mathcal{K}} \alpha_{m,s} = c_m, \quad m = 1, \ldots, \mathcal{K}.$$

3. Set

$$\nu\Theta^{j+1} = \nu\Theta^{j} + \Delta x \sum_{s=1}^{\mathcal{K}} \beta_s f\left(x_j + c_s \Delta x, V^{j,s}, \Theta^{j,s}\right) \tag{7.8}$$

the solution at the next point. Here the coefficients $\beta_s$ are constants with total sum equal to 1, and values of $V^{j,s}$ are computed using interpolation.

The coefficients $\alpha_s$, $\beta_s$ and $c_s$ of the associated with the Runge–Kutta method are usually presented in a matrix form referred as Butcher tableau. That is,

$$\begin{array}{c|cccc} c_1 & \alpha_{1,1} & \alpha_{1,2} & \cdots & \alpha_{1,\mathcal{K}} \\ c_2 & \alpha_{2,1} & \alpha_{2,2} & \cdots & \alpha_{2,\mathcal{K}} \\ \vdots & \vdots & \vdots & & \vdots \\ c_{\mathcal{K}} & \alpha_{\mathcal{K},1} & \alpha_{\mathcal{K},2} & \cdots & \alpha_{\mathcal{K},\mathcal{K}} \\ \hline & \beta_1 & \beta_2 & \cdots & \beta_{\mathcal{K}} \end{array}$$

In our numerical experiments we use the well-known Runge–Kutta–Fehlberg (RKF4(5)) method which allows adaptive stepsize control. For small values of $\nu$ the solution $\Theta$ of the i.v.p (7.1a) might blow up, see the discussion in Section 5.3. Furthermore, as $x \to 1$ we expect the system to be singular since the point $x = 1$ corresponds to the vortex line. In that respect, choosing the stepsize adaptively allows us to capture the correct behaviour of the solution close to the singularity.

### 7.2 Implementation Details

To compute the numerical approximation of the solution for the coupled system (7.1a)–(7.1b), we construct an iterative algorithm and each equation is solved separately using information from the previous iterations. In particular, we follow the following algorithm:

1. Set $V_0^j \equiv V_\infty$, for all $j$
2. For every iterative step $i = 1, \ldots$:

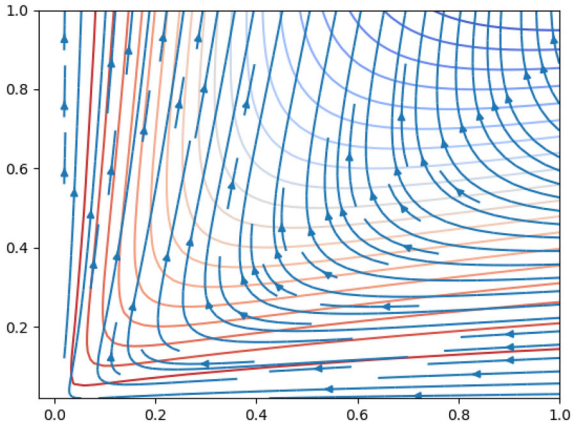


**Fig. 8** (u,w) vector field for $\nu = 0.2$, $E_0 = -0.5$

i. Given $V_{i-1}$, compute $\Theta_i^j$, $\forall\, j$, using the RKF method in [0, 1]
ii. Given $\Theta_i$, compute $V_i^j$, $\forall\, j$, by solving the linear system (7.5)
iii. Solution $(\Theta, V)$ is obtained when the error between two consecutive iterations is small, i.e.

$$\left\{\Delta x \sum_j |V_{i+1}^j - V_i^j|^2\right\}^{\frac{1}{2}} < \epsilon \quad \text{and} \quad \left\{\Delta x \sum_j |\Theta_{i+1}^j - \Theta_i^j|^2\right\}^{\frac{1}{2}} < \epsilon$$

for some $\epsilon > 0$ small.

Note that for the approximation of the integrals in $\mathcal{F}$ we use the composite Simpson's rule.

### 7.3 Numerical Tests

In this section we exhibit numerical approximation of the solution for (7.1a)–(7.1b). We illustrate the results for a different combinations of parameters $\nu$ and $E_0$, while the parameter $V_\infty$ is fixed. For the following examples we take $V_\infty = 1$.

Consider first the case for $\nu = 0.2$ and $E_0 = -0.5$. Then $\Theta(x)$ is positive, and the flow is directed inwards near the plane $z = 0$ and upwards near the vortex line, see Fig. 8.

The converse behaviour, i.e. $\Theta$ is negative, occurs for $\nu = 0.05$ and $E_0 = 0.15$. The flow now has the reverse direction; it is directed outwards near the plane $z = 0$ and downwards near the vortex line, see Fig. 9.

For the parameters $\nu = 0.1$ and $E_0 = -0.2$, the stream function $\Theta$ is first positive and then becomes negative; the flow is directed inwards near the plane $z = 0$ and downwards near the vortex line, see Fig. 10.

The solid lines in Figs. 9, 8 and 10 are the contour lines of the streamfunction $\Theta$.

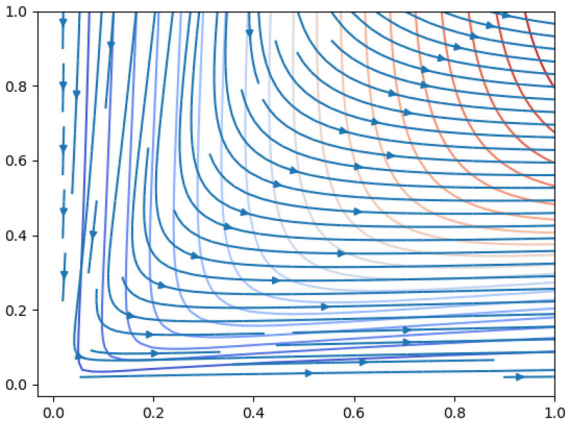


**Fig. 9** (u,w) vector field $\nu = 0.05$, $E_0 = 0.15$

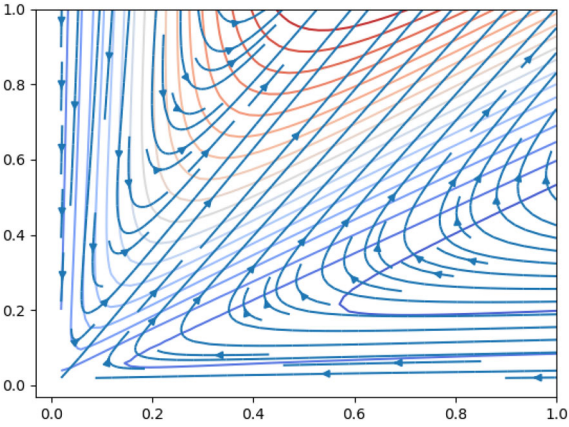


**Fig. 10** (u,w) vector field $\nu = 0.1$, $E_0 = -0.2$

### 7.4 Bifurcation Diagram

We present now a $E_0 - \nu$ bifurcation diagram for (5.16). This diagram is computed using the methodology detailed in Sect. 7.2. To take into account the effect of the parameter $V_\infty$ we consider the following scaled variables:

$$\phi = \frac{V}{V_\infty} \qquad \vartheta = \frac{\Theta}{V_\infty}, \qquad \mu = \frac{\nu}{V_\infty}, \qquad p_0 = \frac{E_0}{V_\infty^2}$$

Then system (7.1a)–(7.2b) becomes

$$\begin{aligned} \mu \frac{\mathrm{d}\vartheta}{\mathrm{d}x} &= \frac{1}{2}\vartheta^2 - \mathcal{F}(x, \phi, p_0), \\ \mu \frac{\mathrm{d}^2\phi}{\mathrm{d}x^2} &= \vartheta \frac{\mathrm{d}\phi}{\mathrm{d}x}, \\ \phi = \vartheta &= 0 \ \text{ at } \ x = 0, \\ \phi &\to 1, \ \text{ as } \ x \to 1, \end{aligned} \tag{7.9}$$

where $\mathcal{F}$ is given by (7.3). The new scaled system exhibits the same behaviour as the original one, so we proceed in identifying numerically the four different zones, see Sect. 5.3:

- *Zone A:* $\vartheta$ is negative
- *Zone B:* $\vartheta$ starts positive and then changes sign
- *Zone C:* $\vartheta$ is positive
- *No Solution:* $\vartheta$ is positive and for small $\mu$ blows up

We take $V_\infty = 1$ and we consider values of $(E_0, \nu) \leftrightarrow (p_0,\ \mu)$ in $\mathcal{B} = [-2, 2] \times [4 \times 10^{-5}, 0.6]$. The set $\mathcal{B}$ is covered initially by $256 = 16 \times 16$ patches $\mathcal{B}_{k,\ell}$ each of size $\delta p_0 \times \delta\mu$. Along the horizontal axis, we take a uniform size $\delta p_0 = 0.25$, while $\delta\mu$ is nonuniform, with a finer grid around $\mu = 4 \times 10^{-5}$ and gradually increasing towards $\mu = 0.6$, with an average $\delta\mu \sim 3.75 \times 10^{-2}$. In each $\mathcal{B}_{k,\ell}$ we consider further a $51 \times 51$ uniform grid of values $\{p_{0_{i,j}}^{k,\ell}, \mu_{i,j}^{k,\ell}\},\ i, j = 1, \ldots, 51$. For all patches and for all values in the patch we identify in which zone the solution belongs to, by solving numerically the scaled system (7.9). The total computational cost of such process is rather small since the work in each patch can be computed independently.

The results of this process are depicted in Fig. 11. On the left graph, the four zones are clearly marked by their boundaries. To distinguish further each zone we "separate" them by shifting slightly each zone along the horizontal axis and Zone C along the vertical axis. On the right graph, the full structure of each zone is now revealed. The boundaries of all zones meet at the point $(p_0, \mu) = (E_0, \nu) = (-\frac{1}{2}, 4 \times 10^{-5}) = (-\beta, 4 \times 10^{-5})$, where $\beta = \frac{\mathrm{d}H}{\mathrm{d}x}(1)$ is the constant appearing in (5.24). For any $E_0 < -\beta$ on the line $\mu = \nu = 4 \times 10^{-5}$ the solution ceases to exist. For larger values of $\nu$, where the solution does exist, the line $E_0 = -\beta$ defines the border between Zone C and Zone B as predicted theoretically, see Sect. 5.3.

A similar diagram appears in Serrin (1972). It uses a slightly different (but equivalent) formulation of the problem, but it is derived through a completely different process. Our bifurcation diagram in Fig. 11 is based on computation of the numerical solution of (5.16) as detailed in the previous paragraph. The diagram of Serrin is a consequence of a series of theoretical estimates and bounds that provide necessary and/or sufficient conditions on the underlying parameters, so that the solutions to the corresponding initial and boundary value problem belong to one of the desired zones; see (Serrin 1972, pp. 349–351). Qualitatively the two diagrams are quite similar, in terms of the overall structure and shape of the borders between the various zones. However, quantitatively there are some differences, due to the different sets of variables and constants used in the two approaches. In our case solutions can exist when the pressure constant $E_0$ is positive, a region which is not addressed in Serrin's work, where solutions are obtained only for negative values of $E_0$. The value $P = 1$ in Serrin (1972, Fig. 1) is the point where all zones converge and beyond this point along the axis $\nu = 0$, solution ceases to exist. In the present work this value corresponds to $E_0 = -\frac{1}{2}$ and the whole diagram is mirrored along this line when compared to that in Serrin (1972, Fig. 1). In both diagrams the two vertical lines define the border between zones B and C. However, it is worth noticing that, apart from having different (opposite) orientations, the curved boundary that separates the *NoSolution* zone from the other zones is very similar in both works.

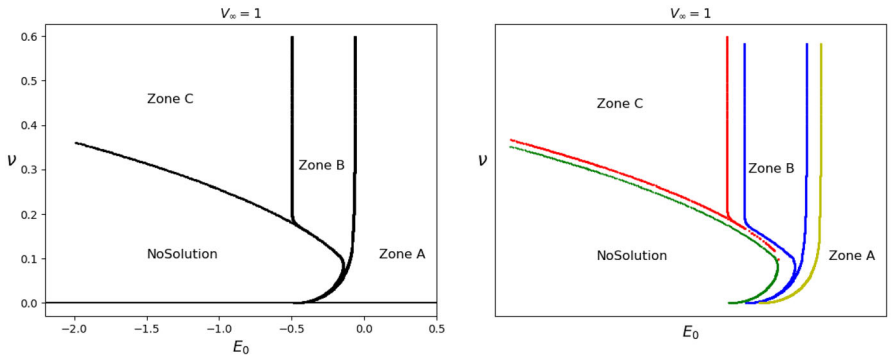


**Fig. 11** $E_0 - \nu$ Bifurcation Diagram

It should be noted that in the diagram in Fig. 11 to the right the borders of the regions have been shifted so that the reader can better visualize the boundaries among the different regions. The actual boundaries in fact overlap as in the diagram to the left.

## 8 Conclusions

This work considers the relation between axisymmetric solutions of the Navier–Stokes and Euler equations. We study stationary self-similar solutions in a setting intended to model tornado-like flows. It is influenced by previous works on this problem by Long (1958, 1961), Goldshtik (1960); Goldshtik and Shtern (1989); Goldshtik (1990) and mainly Serrin (1972) on the interaction of a vortex filament and a plane.

Along with the aforementioned works, it provides a systematic study of stationary self-similar flows focussing on the relation as the viscosity goes to zero. The main findings are: (i) A systematic analysis of exact solutions for the Euler equations which provides an explicit formula for the solution. (ii) Testing the existence of two-cell (or multiple-cell) solutions for the Euler equations and showing that this is not possible. (iii) Providing a rigorous passage from Navier–Stokes to Euler for self-similar solutions (under various hypotheses) in the limit as the viscosity goes to zero. (iv) Presenting a boundary layer analysis via matched asymptotic expansions. (v) Providing a bifurcation diagram via computational methods.

In Serrin (1972), Serrin shows that there are three types of stationary self-similar solutions to the Navier–Stokes equations: (i) a first kind where the radial velocity is directed inwards along the boundary and upwards along the axis of the vortex (corresponds to Fig. 8 and in zone A of the bifurcation diagram of Fig. 11); (ii) a second kind where the radial velocity is directed downwards along the vortex axis and outwards along the boundary (see Fig. 9 corresponding to zone C); (iii) finally, a third kind where the flow is directed downwards on the axis and inwards along the boundary with a compensating outflow in an intermediate angle (see Fig. 10 corresponding to zone B). The last is a flow with two cells. Serrin (1972) posits that solutions of the third kind are important for explaining the central downflow and the cascade effect

frequently observed in tornadoes and provided extensive comparisons with various observational data available at the time.

One motivation of ours was to study how these solutions depend on the viscosity and their persistence in the zero-viscosity limit. We first considered the Euler equations and showed that smooth solutions fall either into the first or the second kind of flows. We then asked if it is possible to have solutions with a slip discontinuity across an interface, this might conceivably correspond to a two-cell solution, but the result was negative. Performing systematic computations that lead to the bifurcation diagram made clear that given the values of $E_0$ and $V_\infty$ solutions in the zone B only appear above a viscosity threshold. They degenerate as the viscosity decreases either because one enters in the region of nonexistence of solutions, or by transitioning from zone B to zone A and in the limit to an exact solution of the Euler system. It may be that the solutions in zone B are indeed related to tornadoes; in that case one should understand how they lose their stability as the viscosity is decreasing.

The stability of the steady self-similar solutions is an open and difficult problem. Another interesting direction of research would be to provide an ansatz that could conceivably produce a moving vortex solution.

## A Navier–Stokes Equations in Cylindrical Coordinates

Cylindrical coordinates $(r, \vartheta, z)$ are connected with rectangular coordinates through the transformation $x_1 = r\ \cos\vartheta, x_2 = r\ \sin\vartheta, x_3 = z$, see Fig. 12, while the associated orthonormal system attached to $P$ is

$$\vec{e}_r = (\cos\vartheta, \sin\vartheta, 0),\ \ \vec{e}_\vartheta = (-\sin\vartheta, \cos\vartheta, 0),\ \ \vec{e}_z = (0, 0, 1).$$

The velocity vector $\vec{u}$ is expressed in cylindrical coordinates as

$$\vec{u} = u(r, \vartheta, z, t)\vec{e}_r + v(r, \vartheta, z, t)\vec{e}_\vartheta + w(r, \vartheta, z, t)\vec{e}_z,$$

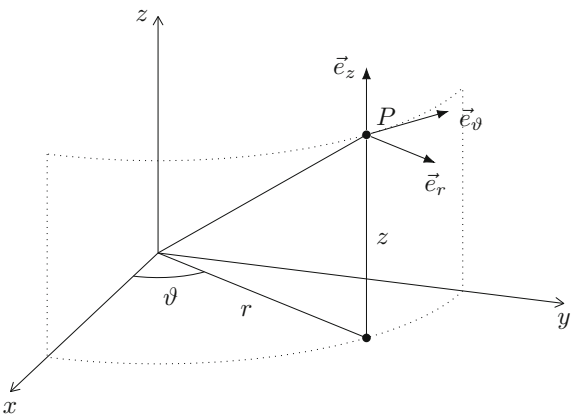


**Fig. 12** Cylindrical coordinate system

while the vorticity $\vec{\omega}$ takes the form

$$\vec{\omega} = \left(\frac{1}{r}\frac{\partial u}{\partial \vartheta} - \frac{\partial v}{\partial z}\right)\vec{e}_r + \left(\frac{\partial u}{\partial z} - \frac{\partial w}{\partial r}\right)\vec{e}_\vartheta + \left(\frac{1}{r}\frac{\partial}{\partial r}(rv) - \frac{1}{r}\frac{\partial w}{\partial \vartheta}\right)\vec{e}_z.$$

A change of variables for the Navier–Stokes equations (2.1) yields the following representation in cylindrical coordinates, see Bird et al. (1987, Table B.2),

$$\frac{\partial u}{\partial t} + (\vec{u}\cdot\nabla)u - \frac{v^2}{r} = -\frac{\partial p}{\partial r} + \nu\Big[\Delta u - \frac{u}{r^2} - \frac{2}{r^2}\frac{\partial v}{\partial \vartheta}\Big], \tag{A.1a}$$

$$\frac{\partial v}{\partial t} + (\vec{u}\cdot\nabla)v + \frac{uv}{r} = -\frac{1}{r}\frac{\partial p}{\partial \vartheta} + \nu\Big[\Delta v - \frac{v}{r^2} + \frac{2}{r^2}\frac{\partial u}{\partial \vartheta}\Big], \tag{A.1b}$$

$$\frac{\partial w}{\partial t} + (\vec{u}\cdot\nabla)w = -\frac{\partial p}{\partial z} + \nu\Delta w, \tag{A.1c}$$

$$\frac{1}{r}\frac{\partial}{\partial r}(ru) + \frac{1}{r}\frac{\partial v}{\partial \vartheta} + \frac{\partial w}{\partial z} = 0. \tag{A.1d}$$

where the operators $\vec{u}\cdot\nabla$ and $\Delta$ are

$$(\vec{u}\cdot\nabla) = u\frac{\partial}{\partial r} + \frac{1}{r}v\frac{\partial}{\partial \vartheta} + w\frac{\partial}{\partial z} \quad \text{and} \quad \Delta = \frac{1}{r}\frac{\partial}{\partial r}\Big(r\frac{\partial}{\partial r}\Big) + \frac{1}{r^2}\frac{\partial^2}{\partial \vartheta^2} + \frac{\partial^2}{\partial z^2}$$

## B Tornadoes

Tornadoes are considered among the most extreme and violent weather phenomena on Earth. They can occur under appropriate circumstances in all continents expect Antarctica, at various seasonal times, and can be hazardous causing loss of human lives and extensive property damage. According to meteorologists, a tornado is defined as a rapidly rotating mass of air that extends downwards from a cumuliform cloud, that is a cloud formed due to vertical motion of air parcels, to the ground. There exist several types of tornadoes, such as landspouts and waterspouts, but the majority of the most destructive tornadoes are known as supercells since their generation takes place within supercell thunderstorms.

Although there is a high interest in forecasting such hazardous tornadoes, it remains a challenging task for researchers to predict when a supercell thunderstorm will lead to a tornado. It is observed that not all supercells are tornadic since a combination of atmospheric instability (caused by the storm) with a wind shear, i.e. a variation of wind speed and direction with altitude, is required for tornado formation. These two ingredients are important for tornado formation; however, the process by which tornadoes are formed is still not fully understood and, thus, difficult to predict. For a detailed presentation on the subject of tornadoes and tornado formation, we refer to Markowski and Richardson (2010, 2014).

### B.1 Modelling Tornadoes

Due to the complexity of tornadoes, the current knowledge about them comes mainly from laboratory experiments and numerical models of idealized supercell thunderstorms, Rotunno (2013). In Ward Ward (1972) conducted a pioneering laboratory experiment reproducing a tornado-like flow considering a fluid with constant density. The idea was to create a flow using a fan that passes through a hole of radius $r_0$ and is placed above a rotating plate in some distance $h$, under the assumption that the ratio of $h/r$ is small. Based on this work, several experimental and numerical simulations have taken place, referred to as Ward-type simulations, Rotunno (2013). It was shown that the vortex form changes as the rotation increases, from single-celled (centerline updraft) to single-celled below to double-celled above, to double-celled (central downdraft surrounded by updraft) to multiple vortices, Rotunno (2013). Also, this structural change is largely independent of the Reynolds number.

Fiedler (1995) proposed an idealization of a tornado-like flow that is defined on a closed domain and is for theoretical analysis. Here, the buoyancy force is taken into consideration. The behaviour of such flows can be analysed numerically using the axisymmetric, incompressible Navier–Stokes equations in cylindrical coordinates. Hence, the model takes the form

$$\frac{Du}{Dt} = \frac{v^2}{r} + 2\Omega v + \frac{1}{Re}\Big[\frac{1}{r}\frac{\partial}{\partial r}\Big(r\frac{\partial u}{\partial r}\Big) + \frac{\partial^2 u}{\partial z^2} - \frac{u}{r^2}\Big] - \frac{\partial p}{\partial r}, \tag{B.1a}$$

$$\frac{Dv}{Dt} = -\frac{uv}{r} - 2\Omega u + \frac{1}{Re}\Big[\frac{1}{r}\frac{\partial}{\partial r}\Big(r\frac{\partial v}{\partial r}\Big) + \frac{\partial^2 v}{\partial z^2} - \frac{v}{r^2}\Big], \tag{B.1b}$$

$$\frac{Dw}{Dt} = b + \frac{1}{Re}\Big[\frac{1}{r}\frac{\partial}{\partial r}\Big(r\frac{\partial w}{\partial r}\Big) + \frac{\partial^2 w}{\partial z^2}\Big] - \frac{\partial p}{\partial z}, \tag{B.1c}$$

$$0 = \frac{1}{r}\frac{\partial}{\partial r}(ru) + \frac{\partial w}{\partial z}, \tag{B.1d}$$

where $\frac{D}{Dt} = \frac{\partial}{\partial t} + u\frac{\partial}{\partial r} + w\frac{\partial}{\partial z}$ stands for the material derivative, $b$ is the buoyancy and $\Omega$ is the nondimensional swirl ratio which depends on both the angular momentum and the buoyancy. Numerical experiments of this model produce results analogous to Ward-type experiments for different values of $\Omega$ and $Re$, Rotunno (2013).

In addition, various analytical models have been introduced to describe a tornado-like flow behaviour. Assuming that a vortex line resembles the tornado core, we consider again the incompressible axisymmetric Euler and Navier–Stokes equations.

Let us review some widely used vortex models. A detailed presentation can be found in Gillmeier et al. (2018) and Kim and Matsui (2017) and in references therein.

The Rankine vortex model is considered as the simplest one. Here the flow is assumed to be one-dimensional, steady, inviscid and all body forces are omitted. Hence, the model takes the form

$$\frac{\mathrm{d}p(r)}{\mathrm{d}r} = \rho\frac{v^2}{r},$$

where $\rho$ is the density. Also, it is assumed that the velocity component is discontinuous and is written as

$$\bar{v}(\bar{r}) = \begin{cases} \bar{r} & for\ \bar{r} < 1, \\ \dfrac{1}{\bar{r}} & for\ \bar{r} > 1. \end{cases}$$

where $\bar{v} = \frac{v}{v_{\max}}$ is the normalized velocity and $\bar{r} = \frac{r}{R}$ is the normalized distance for $R$ the radius of the core vortex. Sometimes, a modified version of velocity is used that is

$$\bar{v} = \frac{2\bar{r}}{(1+\bar{r}^2)}.$$

If the discontinuous velocity is considered, solving the differential equation yields the normalized pressure $\bar{p}(\bar{r}) = \frac{p(r)}{\rho v_{\max}^2}$ that is

$$\bar{p}(\bar{r}) = \begin{cases} \bar{p}(0) + \dfrac{1}{2}\bar{r}^2 & for\ \bar{r} < 1, \\ \bar{p}|_{r\to\infty} - \dfrac{1}{\bar{r}^2} & for\ \bar{r} > 1. \end{cases}$$

Another vortex model is the Burgers–Rott, where the flow is assumed to be steady, with constant viscosity and zero body forces. Moreover, it is assumed that $u = u(r)$, $v = v(r)$, $w = w(z)$ and $p = p(r, z)$. The model then has the following form

$$u\frac{\partial u}{\partial r} - \frac{v^2}{r} = \mu\Big[\frac{1}{r}\frac{\partial}{\partial r}\Big(r\frac{\partial u}{\partial r}\Big) - \frac{u}{r^2}\Big] - \frac{1}{\rho}\frac{\partial p}{\partial r}, \tag{B.2a}$$

$$u\frac{\partial v}{\partial r} + \frac{uv}{r} = \mu\Big[\frac{1}{r}\frac{\partial}{\partial r}\Big(r\frac{\partial v}{\partial r}\Big) - \frac{v}{r^2}\Big], \tag{B.2b}$$

$$w\frac{\partial w}{\partial z} = -\frac{1}{\rho}\frac{\partial p}{\partial z}, \tag{B.2c}$$

$$\frac{1}{r}\frac{\partial}{\partial r}(ru) + \frac{\partial w}{\partial z} = 0, \tag{B.2d}$$

where $\rho$ is the density and $\mu$ the dynamic viscosity. It is also assumed that

$$\bar{w}(\bar{z}) = 2\,\alpha\,\bar{z},$$
$$\bar{u}(\bar{r}) = -\alpha\,\bar{r},$$

where $\bar{z} = \frac{z}{R}$ is the normalized vertical height, $\bar{u} = \frac{u}{v_{\max}}$ and $\bar{w} = \frac{w}{v_{\max}}$ are the normalized velocities and $\alpha = \frac{2\mu}{v_{\max}}$. Under these assumptions, solving the system (B.2) implies the following

$$\bar{v}(\bar{r}) = \frac{1}{\bar{r}}(1 - exp(-\bar{r}^2)), \quad \text{and}$$

$$\bar{p}(\bar{r},\bar{z}) = \bar{p}(0,0) + \int_0^{\bar{r}} \frac{\bar{v}^2(s)}{s}\mathrm{d}s - \frac{\bar{\alpha}}{2}(\bar{r}^2 + 4\bar{z}^2)$$

The Sullivan vortex model has also been used widely to model tornado-like flows. As in the case of the Burgers–Rott model, we consider a flow that is stationary, with constant viscosity and zero body forces. In addition, it is considered that velocity components are given in the form $u = u(r)$, $v = v(r)$, $w = w(r,z)$, while pressure is of the form $p = p(r,z)$. One may conclude to the following

$$\begin{aligned}
\bar{u}(\bar{r}) &= -\bar{\alpha}\bar{r} + \frac{2b\bar{v}}{\bar{r}}(1 - e^{-\bar{r}^2}),\\
\bar{v}(\bar{r}) &= \frac{1}{\bar{r}}\frac{H(x)}{H(\infty)},\\
\bar{w}(\bar{r},\bar{z}) &= 2\bar{\alpha}\bar{z}(1 - b\,e^{-\bar{r}^2}),
\end{aligned}$$

where $H(x) = \int_0^x e^{-s+3\int_0^s \frac{1}{\sigma}(1-e^{-\sigma^2})\mathrm{d}\sigma}\mathrm{d}s$ for $x = \bar{r}^2$. It is worth mentioning that although the Sullivan and the Burgers–Rott models have some similarities, the Sullivan model allows the generation of a double-celled vortex, while Burgers–Rott model does not.

### B.2 Mathematical Approach

A theoretically sound approach towards study of tornadoes was introduced by Long (1958, 1961). Assuming the tornado core is modelled by a semi-infinite vortex line in a fluid interacting with a plane boundary surface, he presented the reduction of incompressible Navier–Stokes equations to a system of differential equations motivated by boundary layer theory. Several subsequent studies (Hall 1972; Burggraf and Foster 1977; Shtern and Hussain 1999; Shtern 2012) took a similar direction and studied the formation of a boundary layer considering the near-axis boundary layer approximation to the incompressible axisymmetric Navier–Stokes equations. This is usually referred as quasi-cylindrical approximation and leads to the system

$$\begin{aligned}
\frac{v^2}{r} &= \frac{\partial p}{\partial r},\\
u\frac{\partial v}{\partial r} + w\frac{\partial v}{\partial z} + \frac{uv}{r} &= \nu\Big[\frac{1}{r}\frac{\partial}{\partial r}\Big(r\frac{\partial v}{\partial r}\Big) - \frac{v}{r^2}\Big],\\
u\frac{\partial w}{\partial r} + w\frac{\partial w}{\partial z} &= \nu\Big[\frac{1}{r}\frac{\partial}{\partial r}\Big(r\frac{\partial w}{\partial r}\Big)\Big] - \frac{\partial p}{\partial z},\\
\frac{1}{r}\frac{\partial}{\partial r}(ru) + \frac{\partial w}{\partial z} &= 0,
\end{aligned}$$

The boundary layer is associated in the literature with the vortex breakdown that is the change of direction of the flow near the boundary as $\nu \to 0$.

Independently, Goldshtik (1960) showed that a similar reduction of incompressible axisymmetric Navier–Stokes equations to a system of differential equations leads

to a 'paradoxical' exact solution that vanishes for some values of Reynolds number, Goldshtik (1960). Serrin (1972) broadened this class of solutions and described the existence of three different solution profiles depending on an arbitrary parameter and the kinematic viscosity, Serrin (1972). Following this work, several authors have extended the study to the generalized case of conical flows, Shtern and Hussain (1999), Fernandez-Feria and Arrese (2000), Shtern (2012). The ideas of Long and Goldshtik have been applied to investigate the formation of a boundary layer and the loss of existence of such solutions using different boundary conditions or a modified self-similar ansatz, Hall (1972), Burggraf and Foster (1977), Goldshtik (1990), Goldshtik and Shtern (1989, 1990). This line of research is systematized in the present manuscript by studying stationary solutions of the axisymmetric Navier–Stokes equations.

The above References concern the interaction of a vortex with a boundary when the flow is assumed stationary. Models have been devised concerning the motion of the vortex core structure and its coupling with environmental flows, and the reader is referred to Paeschke et al. (2012), Lunasin et al. (2016) and references therein regarding that subject.

**Acknowledgements** Research was partially supported by King Abdullah University of Science and Technology (KAUST) (Grant No. BAS/1/1652-01-01) baseline funds.

## Declarations

**Conflict of interest** The authors have no conflict of interest to report.

## References

Bird, R.B., Armstrong, R.C., Hassager, O.: Dynamics of Polymeric Liquids. Fluid Mechanics, vol. 1. Wiley, London (1987)
Brezis, H.: Functional Analysis. Sobolev Spaces and Partial Differential Equations. Universitext. Springer, New York (2010)
Burggraf, O.R., Foster, M.R.: Continuation or breakdown in tornado-like vortices. J. Fluid Mech. **80**(4), 685–703 (1977)
Bělík, P., Dokken, D.P., Scholz, K., Shvartsman, M.M.: Fractal powers in Serrin's swirling vortex solutions. Asymptot. Anal. **90**, 53–82 (2014)
Fernandez-Feria, R., Arrese, J.C.: Boundary layer induced by a conical vortex. Q. J. Mech. Appl. Math. **53**(4), 609–628 (2000)
Fernandez-Feria, R., Fernandez de la mora, J., Barrero, A.: Solution breakdown in a family of self-similar nearly inviscid axisymmetric vortices. J. Fluid Mech. **305**, 77–91 (1995)
Fiedler, H.B.: On modelling tornadoes in isolation from the parent storm. Atmos. Ocean **33**(3), 501–512 (1995)
Folland, G.: Real Analysis: Modern Techniques and Their Applications. Pure and Applied Mathematics: A Wiley Series of Texts, Monographs and Tracts. Wiley, London (2013)
Gillmeier, S., Sterling, M., Hemida, H., Baker, C.: A reflection on analytical tornado-like vortex flow field models. J. Wind Eng. Ind. Aerodyn. **174**, 10–27 (2018)
Goldshtik, M.: A paradoxical solution of the Navier–Stokes equations. J. Appl. Math. Mech. **24**(4), 913–929 (1960)
Goldshtik, M.A.: Viscous-flow paradoxes. Annu. Rev. Fluid Mech. **22**(1), 441–472 (1990)
Goldshtik, M., Shtern, V.: Analysis of the paradox of the interaction of a vortex filament with a plane. J. Appl. Math. Mech. **53**(3), 319–325 (1989)
Goldshtik, M.A., Shtern, V.N.: Collapse in conical viscous flows. J. Fluid Mech. **218**, 483–508 (1990)
Hall, M.: Vortex breakdown. Annu. Rev. Fluid Mech. **4**(1), 195–218 (1972)

Holmes, M.H.: Introduction to Perturbation Methods, vol. 20, 2nd edn. Springer, New York (2013)
Holmes, M.H., Stein, F.M.: Sturmian theory and transformations for the Riccati equation. Port. Math. **35**, 1–2 (1976)
Kim, Y.C., Matsui, M.: Analytical and empirical models of tornado vortices: a comparative study. J. Wind Eng. Ind. Aerodyn. **171**, 230–247 (2017)
Lagerstrom, P.A.: Matched Asymptotic Expansions: Ideas and Techniques, vol. 76. Springer, New York (1988)
Long, R.R.: Vortex motion in a viscous fluid. J. Atmos. Sci. **15**(1), 108–112 (1958)
Long, R.R.: A vortex in an infinite viscous fluid. J. Fluid Mech. **11**(4), 611–624 (1961)
Lunasin, E., Malek-Madani, R., Slemrod, M.: A dynamical systems approach to mathematical modeling of tornadoes. Bull. Inst. Math. Acad. Sin. (N.S.) **11**(1), 145–161 (2016)
Majda, A.J., Bertozzi, A.L.: Vorticity and Incompressible Flow. Cambridge Texts in Applied Mathematics. Cambridge University Press, Cambridge (2001)
Markowski, P., Richardson, Y.: Hazards Associated with Deep Moist Convection, pp. 273–313. Wiley, London (2010)
Markowski, P., Richardson, Y.: What we know and don't know about tornado formation. Phys. Today **67**(9), 26–31 (2014)
Morton, B.: Geophysical vortices. Prog. Aerosp. Sci. **7**, 145–194 (1966)
Paeschke, E., Marschalik, P., Owinoh, A., Klein, R.: Motion and structure of atmospheric mesoscale baroclinic vortices: dry air and weak environmental shear. J. Fluid Mech. **701**, 137–170 (2012)
Papadoperakis, I.: Weak star limits of probability measures of special type. Math. Proc. Camb. Philos. Soc. **127**(1), 173–191 (1999)
Rotunno, R.: The fluid dynamics of tornadoes. Annu. Rev. Fluid Mech. **45**(1), 59–84 (2013)
Serrin, J.: The swirling vortex. Philos. Trans. R. Soc. Lond. Ser. A Math. Phys. Sci. **271**, 325–360 (1972)
Shtern, V.: Counterflows: Paradoxical Fluid Mechanics Phenomena. Cambridge University Press, Cambridge (2012)
Shtern, V., Hussain, F.: Collapse, symmetry breaking, and hysteresis in swirling flows. Annu. Rev. Fluid Mech. **31**(1), 537–566 (1999)
Sozou, C.: On solutions relating to conical vortices over a plane wall. J. Fluid Mech. **244**, 633–644 (1992)
Sozou, C., Wilkinson, L.C., Shtern, V.N.: On conical swirling flows in an infinite fluid. J. Fluid Mech. **276**, 261–271 (1994)
Tzavaras, A.E.: Wave structure induced by fluid-dynamic limits in the Broadwell model. Arch. Ration. Mech. Anal. **127**, 361–387 (1994)
Tzavaras, A.E.: Wave interactions and variation estimates for self-similar zero-viscosity limits in systems of conservation laws. Arch. Ration. Mech. Anal. **135**(1), 1–60 (1996)
Ward, N.B.: The exploration of certain features of tornado dynamics using a laboratory model. J. Atmos. Sci. **29**(6), 1194–1204 (1972)